

## A SIMPLE AND UNIFIED ONE-DIMENSIONAL MODEL TO DESCRIBE VARIOUS CHARACTERISTICS OF SOILS

TERUO NAKAI<sup>i)</sup>, HOSSAIN MD. SHAHIN<sup>ii)</sup>, MAMORU KIKUMOTO<sup>iii)</sup>,  
HIROYUKI KYOKAWA<sup>iv)</sup>, FENG ZHANG<sup>v)</sup> and MARCIO M. FARIAS<sup>vi)</sup>

### ABSTRACT

A simple and unified constitutive model for soils, considering various effects such as the influences of density, bonding, time dependent behavior and others, is presented in this paper. The elastoplastic behavior of over consolidated non-structured soils under a one-dimensional stress condition is firstly presented by introducing a state variable that represents the influence of density (stage I). To describe the one-dimensional stress-strain behavior of structured soils, attention is focused on density and bonding as the main factors that affect the response of this type of soil, because it can be considered that soil skeleton structure which is in a looser state than that of a normally consolidated soil is formed by bonding effects (stage II). Furthermore, a simple method is presented which allows for other soil characteristics to be considered, such as time and temperature dependency, and the effect of suction in unsaturated soils. Experimental observations show that the normally consolidated line (NCL) in the void ratio—stress relation (e.g.,  $e$ - $\ln \sigma$  curve) shifts depending on the change of strain rate, temperature, suction and others (stage III). The validation of the model at stages I and II is demonstrated by simulating one-dimensional consolidation tests for normally consolidated, over consolidated and natural clays. The applicability of the model at stage III is verified not only by the simulations of time-dependent behavior of clays in one-dimensional element tests but also by the soil-water coupled finite element analysis of oedometer tests as a boundary value problem. The extension from one-dimensional models to three-dimensional models is easily achieved by defining the yield function using stress invariants instead of one-dimensional stress ' $\sigma$ ' and by assuming an appropriate flow rule in stress space. The details of the modeling in general three-dimensional stress conditions will be described in another paper (Nakai et al., 2011).

**Key words:** aging, bonding, clay, consolidation, constitutive equation of soil, deformation, density, elasto-plasticity, one-dimensional condition, overconsolidation, rheology, sand, structured soil, (suction effect), (temperature-dependent behavior), (time-dependent behavior) (IGC: D5/D6)

### INTRODUCTION

Constitutive models for geomaterials try to predict the deformation and failure of the ground subjected to the forces imposed by geotechnical structures. Therefore, models which are developed to simulate the behavior of a limited number of materials or those tested under limited stress conditions may not be useful in practical design.

The Cam clay model (e.g., Schofield and Wroth, 1968), which was developed almost 50 years ago, was an epoch-making constitutive model for geomaterials. This is because the model proposed a unified framework to describe the consolidation and shear behaviors of unstructured clays, which had been investigated separately before that time. However, the Cam clay model cannot

properly predict the soil behavior except for remolded normally consolidated clay under the conventional axis-symmetric triaxial compression condition. Although many constitutive models have been proposed to overcome the limitations of the Cam clay model, most of them are complex, and/or the conditions to which they can be applied are still restricted. The features of geomaterials which are not taken into consideration in the Cam clay model are as follows:

- (1) Influence of intermediate principal stress on the deformation and strength of geomaterials;
- (2) Dependency of the direction of plastic flow on the stress path;
- (3) Positive dilatancy during strain hardening;
- (4) Stress induced anisotropy and cyclic loading;

<sup>i)</sup> Professor, Department of Civil Engineering, Nagoya Institute of Technology, Nagoya, Japan (nakai.teruo@nitech.ac.jp).

<sup>ii)</sup> Associate professor, ditto.

<sup>iii)</sup> Assistant professor, ditto.

<sup>iv)</sup> Graduate student, ditto (now JSPS postdoctoral fellow, IIS, University of Tokyo).

<sup>v)</sup> Professor, ditto.

<sup>vi)</sup> Professor, Department of Civil and Environmental Engineering, University of Brasilia, Brazil.

The manuscript for this paper was received for review on November 10, 2010; approved on July 13, 2011.

Written discussions on this paper should be submitted before July 1, 2012 to the Japanese Geotechnical Society, 4-38-2, Sengoku, Bunkyo-ku, Tokyo 112-0011, Japan. Upon request the closing date may be extended one month.

- (5) Inherent anisotropy;
- (6) Influence of density and/or confining pressure on the deformation and strength;
- (7) Behavior of structured soils such as naturally deposited clay;
- (8) Time-dependent behavior and rheological characteristics;
- (9) Temperature-dependent behavior;
- (10) Behavior of unsaturated soils;
- (11) Influence of particle crushing.

In the 1980's, two simple constitutive models for clay and sand were developed: one is referred to as the  $t_{ij}$ -clay model (Nakai and Matsuoka, 1986) and the other is referred to as the  $t_{ij}$ -sand model (Nakai, 1989). In these models, "(1) the influence of intermediate principal stress on the deformation and strength" is considered with the adaption of the concept of modified stress  $t_{ij}$  into consideration (Nakai and Mihara, 1984), and "(2) the stress path dependency of plastic flow" is considered with the introduction of the plastic strain increment division into two components: a plastic strain increment which satisfies an associated flow rule in the  $t_{ij}$  space and an isotropic plastic strain increment due to increasing mean stress. Later, these models based on the  $t_{ij}$  concept were integrated into the unique model named subloading  $t_{ij}$  model (Nakai and Hinokio, 2004), in which "(3) Positive dilatancy during strain hardening" and "(6) Influence of density and/or confining pressure on the deformation and strength" are taken into consideration by introducing and revising the subloading surface concept (Hashiguchi and Ueno, 1977; Hashiguchi, 1980). Furthermore, by referring to the concept of a superloading surface as well as a subloading surface from Asaoka and collaborators (Asaoka et al, 2000a; Asaoka, 2003) and modifying it, the subloading  $t_{ij}$  model was extended to also describe "(7) the behavior of structured soil such as naturally deposited clay" (Nakai, 2007, Nakai et al., 2009a).

In the present paper, a simple and unified framework to take several of the above-mentioned features into account will be described. The modeling of these features is initially developed under one-dimensional conditions to provide an easy framework for the basic ideas of how to account for the influence of density, the bonding effect and other features, such as time-dependent behavior. Some of the present modeling is described in a paper on applied mechanics in Japanese as well (Nakai et al., 2009b). Three-dimensional models can easily be developed by extending these one-dimensional models using the  $t_{ij}$  concept.

## DESCRIPTION OF ONE-DIMENSIONAL BEHAVIOR OF NORMALLY CONSOLIDATED SOIL BY CONVENTIONAL ELASTOPLASTICITY

In this section, the well known relation between the stress and void ratio of soil under one-dimensional conditions is formulated using a simple approach that will set the basis for further developments of the proposed

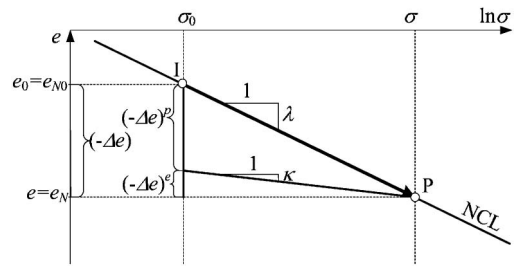


Fig. 1. Change of void ratio in a normally consolidated (NC) clay

model. Figure 1 shows the typical relation between void ratio ( $e$ ) and stress in logarithmic scale ( $\ln \sigma$ ) for a normally consolidated clay, as described in many soil mechanics text books. Here, point I ( $\sigma = \sigma_0$ ,  $e = e_0$ ) represents the initial state, and point P ( $\sigma = \sigma$ ,  $e = e$ ) represents the current state. The symbols  $e_{N0}$  and  $e_N$  denote the void ratios on the normally consolidated line (NCL) at the initial stress and at the current stress, respectively. The slopes  $\lambda$  and  $\kappa$  of the straight lines denote the compression and swelling indices, respectively. When the stress state moves from  $\sigma_0$  to  $\sigma$ , the total finite change in void ratio ( $-\Delta e$ ) of a normally consolidated clay is expressed as:

$$(-\Delta e) = e_0 - e = e_{N0} - e_N = \lambda \ln \frac{\sigma}{\sigma_0} \quad (1)$$

and its elastic (recoverable) component  $(-\Delta e)^e$  is computed using the swelling index  $\kappa$  as follows:

$$(-\Delta e)^e = \kappa \ln \frac{\sigma}{\sigma_0} \quad (2)$$

The plastic (irrecoverable) component  $(-\Delta e)^p$  is then given by:

$$(-\Delta e)^p = (-\Delta e) - (-\Delta e)^e = \lambda \ln \frac{\sigma}{\sigma_0} - \kappa \ln \frac{\sigma}{\sigma_0} \quad (3)$$

Now, let  $F$  and  $H$  denote the following terms related to the logarithmic change of stress and the change in plastic void ratio, respectively;

$$F = (\lambda - \kappa) \ln \frac{\sigma}{\sigma_0} \quad (4)$$

$$H = (-\Delta e)^p \quad (5)$$

The term  $F$  is a scalar function of the stress state, and the change in plastic void ratio  $H = (-\Delta e)^p$  can be considered as the strain hardening parameter. Rewriting Eq. (3) in terms of these variables, the yield function  $f$  for a normally consolidated soil in one-dimensional condition can be expressed as:

$$F = H \quad \text{or} \quad f = F - H = 0 \quad (6)$$

Figure 2 shows the graphical representation of the relation between  $F$  and  $H$  given by Eq. (6). This can be interpreted as a hardening rule. The change in the plastic void ratio relates to the stress function  $F$  according to a straight line with a unitary slope, so that the stress point is always on the yield surface. Then consistency condition

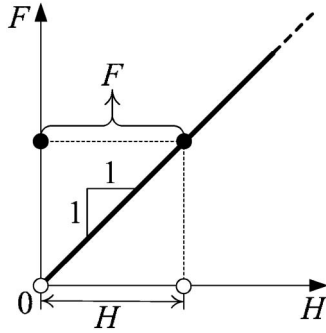


Fig. 2. Evolution of  $F$  and  $H$  in a normally consolidated (NC) soil

( $df=0$ ) gives:

$$df = dF - dH = (\lambda - \kappa) \frac{d\sigma}{\sigma} - d(-e)^p = 0 \quad (7)$$

Therefore, the infinitesimal increment of plastic void ratio is expressed as:

$$d(-e)^p = (\lambda - \kappa) \cdot \frac{d\sigma}{\sigma} \quad (8)$$

This relation could also be obtained directly by differentiating Eq. (3). On the other hand, differentiating Eq. (2), the infinitesimal increment of elastic void ratio is expressed as follows:

$$d(-e)^e = \kappa \frac{d\sigma}{\sigma} \quad (9)$$

The increment of total void ratio is given by the summation of Eqs. (8) and (9) is expressed as an elastoplastic relation in the form

$$d(-e) = d(-e)^p + d(-e)^e = \{(\lambda - \kappa) + \kappa\} \frac{d\sigma}{\sigma} \quad (10)$$

The approach described above will be used in the following sections, in order to introduce the influence of other relevant characteristics that affect the behavior of real soils.

**ONE-DIMENSIONAL MODELING OF OVER CONSOLIDATED SOIL BASED ON ADVANCED ELASTOPLASTICITY (STAGE I)**

The simple relation in Eq. (10) describes well the behavior of remolded clays normally consolidated under one-dimensional or isotropic compression. This type of relation is assumed in the well known Cam clay model. Under those hypotheses, such a remolded clay in a over consolidated state, i.e., for a current stress smaller than the yield stress, behaves according to a linear  $e$ - $\ln \sigma$  relation with constant inclination,  $\kappa$ . This actually means a nonlinear elastic behavior under unloading and reloading. Nevertheless, real clays show elastoplastic behavior even in the over consolidation region. Figure 3 shows schematically the  $e$ - $\ln \sigma$  relation for over consolidated soils. Even in the over consolidation region, elastoplastic deformation occurs, and the void ratio of the soil grad-

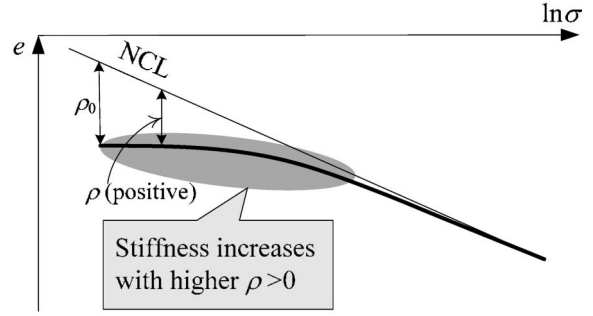


Fig. 3. Void ratio ( $e$ ):  $\ln \sigma$  relation in over consolidated (OC) clays

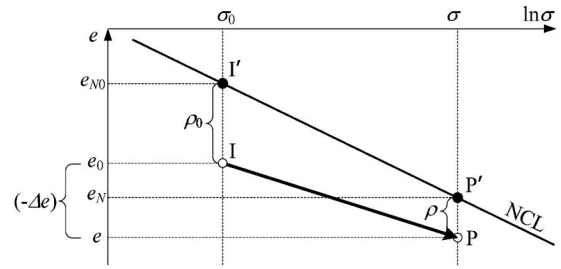


Fig. 4. Change of void ratio in an over consolidated (OC) clay

ually approaches the normally consolidated line (NCL) with increasing stress.

Figure 4 shows the total or finite change of the void ratio ( $-\Delta e$ ) when the stress condition moves from the initial state I ( $\sigma = \sigma_0$ ) to the current state P ( $\sigma = \sigma$ ). Here,  $e_0$  and  $e$  are the initial and current void ratios of the over consolidated soil, whereas  $e_{N0}$  and  $e_N$  denote the corresponding void ratios for virtual points I' and P' on the normally consolidated line (NCL). The difference between the void ratio ( $e_N$ ) for the virtual point on the NCL and the actual void ratio ( $e$ ), for the same stress level, will be denoted as  $\rho$ . This variable represents an increase in the void ratio, and therefore in density, for the over consolidated remolded soil with respect to the density at a normally consolidated condition. Hence, the value of  $\rho$  is always positive for unstructured over consolidated soils, and under this condition, the soil is denser and presents a higher stiffness, as illustrated in Fig. 3. Variable  $\rho$  also represents a measure of over consolidation and can be easily related to the over consolidation ratio (OCR) as:

$$\rho = (\lambda - \kappa) \ln(\text{OCR}) \quad (11)$$

When the actual stress level increases, the soil becomes less over consolidated, and the value of  $\rho$  decreases and tends to zero as the  $e$ - $\ln \sigma$  relation approaches the normally consolidated line.

By referring again to Fig. 4, note that when the stress condition moves from the initial state I to the current state P, the difference of void ratios between the normally consolidated and over consolidated conditions for the same stress state is expressed as the change from  $\rho_0 (= e_{N0} - e_0)$  to  $\rho (= e_N - e)$ . The total or finite change in the void ratio ( $-\Delta e$ ) can be easily computed as:

$$\begin{aligned}
(-\Delta e) &= e_0 - e \\
&= (e_{N0} - \rho_0) - (e_N - \rho) \\
&= (e_{N0} - e_N) - (\rho_0 - \rho)
\end{aligned} \quad (12)$$

Here, it will be assumed that the recoverable change in the void ratio  $(-\Delta e)^e$  (elastic component) for over consolidated soils is the same as that for normally consolidated soils, which is given by Eq. (2). Then, referring to Fig. 4 and Eq. (12), the plastic change in void ratio  $(-\Delta e)^p$  for over consolidated soils is obtained as:

$$\begin{aligned}
(-\Delta e)^p &= (-\Delta e) - (-\Delta e)^e \\
&= \{(e_{N0} - e_N) - (\rho_0 - \rho)\} - (-\Delta e)^e \\
&= \lambda \ln \frac{\sigma}{\sigma_0} - (\rho_0 - \rho) - \kappa \ln \frac{\sigma}{\sigma_0}
\end{aligned} \quad (13)$$

From this equation and using the definitions of  $F$  and  $H$  in Eqs. (4) and (5), the yield function for over consolidated soils is expressed as follows:

$$F + \rho = H + \rho_0 \quad \text{or} \quad f = F - \{H + (\rho_0 - \rho)\} = 0 \quad (14)$$

From the consistency condition ( $df=0$ ) during the occurrence of plastic deformation and satisfying Eq. (14), the following equation is obtained:

$$\begin{aligned}
df &= dF - \{dH - d\rho\} \\
&= (\lambda - \kappa) \frac{d\sigma}{\sigma} - \{d(-e)^p - d\rho\} = 0
\end{aligned} \quad (15)$$

Two internal strain-like variables  $H$  and  $\rho$  control the (isotropic) hardening of the model. This is schematically illustrated by the solid line in Fig. 5, which represents the relation between  $F$  and  $(H + \rho_0)$  for an over consolidated soil as expressed in Eq. (14). This line approaches the broken line ( $F=H$ ) of normally consolidated soils with the development of plastic deformation. The solid curve is shifted by  $\rho_0$  to the right of the origin, which represents the accumulated plastic void ratio reduction, to bring the soil from a normally consolidated condition to the actual over consolidated state. Here, the horizontal distance between the solid line and the broken line indicates the current density variable  $\rho$ , which decreases with the development of plastic deformation and tends to zero as the soil approaches the normally consolidated state. The slope  $dF/dH$  of the solid line gives an idea of the stiffness

against the plastic change in the void ratio for over consolidated soils. This can be compared with the stiffness of a normally consolidated soil given by the slope  $dF/dH$  of the broken line, which is always unity in this diagram.

It is necessary to formulate an evolution rule for the internal variable  $\rho$ , which represents the density. It can be assumed that the state variable  $\rho$  decreases ( $d\rho < 0$ ) with the development of plastic deformation (volume contraction)—i.e.  $d\rho \propto d(-e)^p$ —and finally becomes zero in the normally consolidated state. Furthermore, it can be considered that  $d\rho$ , the degree of degradation of  $\rho$ , decreases as the value of  $\rho$  becomes small. This can be expressed by means a function  $G(\rho)$ . In order to fulfill the conditions above, the function  $G(\rho)$  must decrease monotonically and satisfy  $G(0)=0$  in order to adhere to the normally consolidated line (NCL). Therefore, the evolution rule of  $\rho$  can be given in the following general form:

$$d\rho = -G(\rho) \cdot d(-e)^p \quad (16)$$

By substituting Eq. (16) into (15), the infinitesimal increment of plastic void ratio is given by:

$$d(-e)^p = \frac{\lambda - \kappa}{1 + G(\rho)} \cdot \frac{d\sigma}{\sigma} \quad (17)$$

Then, the increment of total void ratio is expressed as follows from Eqs. (9) and (17):

$$d(-e) = d(-e)^p + d(-e)^e = \left\{ \frac{\lambda - \kappa}{1 + G(\rho)} + \kappa \right\} \frac{d\sigma}{\sigma} \quad (18)$$

As seen from the above equation,  $G(\rho)$  has the effect of increasing the stiffness of the soil, and this effect becomes larger with the increase of the value of  $\rho$ . A value  $G(\rho) = 0.2$ , for instance, represents an increase of 20% in the plastic component of the stiffness, compared to that of a normally consolidated soil. After  $G(\rho)$  becomes zero for vanishing values of  $\rho$ , then Eq. (18) corresponds to Eq. (10), which is the formulation for normally consolidated soils. The method used here to consider the influence of density corresponds somewhat to an interpretation of the subloading surface concept by Hashiguchi (1980) under one-dimensional conditions.

## ONE-DIMENSIONAL MODELING OF STRUCTURED SOIL BASED ON ADVANCED ELASTOPLASTICITY (STAGE II)

The model developed in the previous section can represent quite well the behavior of over consolidated remolded clays, as will be demonstrated later. However, natural clays behave intricately compared with remolded clays which are used in laboratory tests, because natural clays develop a complex structure during their deposition process. Such structured soils can exist naturally with a void ratio greater than that of a non-structured normally consolidated soil under the same stress condition, yet the structured soil may have a higher stiffness due to natural cementation. Due to debonding effects, this type of structured soil shows a rather brittle and more compressive behavior than non-structured soils after reaching a certain

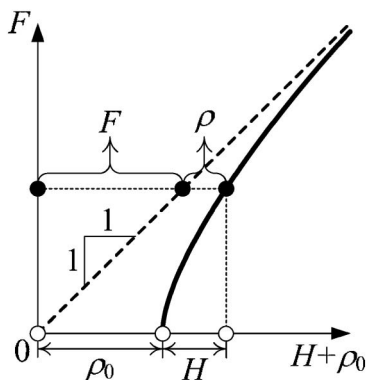


Fig. 5. Evolution of  $F$  and  $H$  in an over consolidated (OC) soil

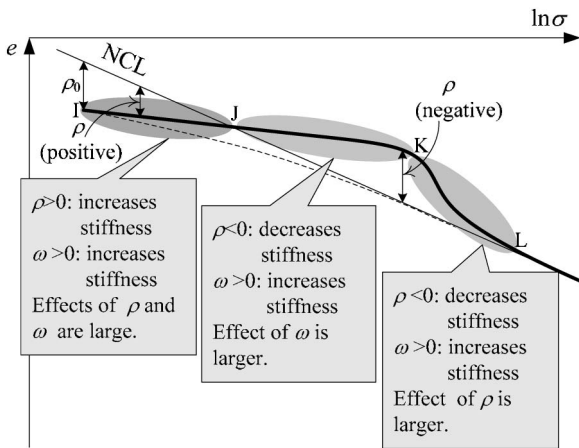


Fig. 6. Void ratio ( $e$ ):  $\ln \sigma$  relation in structured clays

stress level. This is illustrated by the solid curve in Fig. 6, which shows schematically a typical  $e$ - $\ln \sigma$  relation for natural clays. Three regions may be identified in this figure: in region I, from point I to J, the stress level is low and the structured soil presents a denser ( $\rho > 0$ ) and stiffer state than the NCL; in region II, from point J to K, the structured soil is in a looser ( $\rho < 0$ ) yet stiffer state than the NCL; in region III, from point K to L, the stress level is such that debonding effects prevails and the structure collapses fast with the corresponding changes in stiffness. Finally the curve of the real soil approaches the NCL from above. Compare this with the thin broken curve of a non-structured over consolidated soil which approaches the NCL from below, in the same figure.

Asaoka et al. (2002) and Asaoka (2003) developed a model to describe such structured soils, introducing the concepts of subloading and superloading surfaces to the Cam-clay model. In their modeling, a factor related to the over consolidation ratio was introduced to increase the initial stiffness, and a factor related to the soil skeleton structure was introduced to decrease the stiffness as the stress state approached the normally consolidated condition. By controlling the evolution rules of these factors, they described various features of consolidation and shear behaviors of structured soils.

In the present paper, attention is focused in the real density and the bonding as the main factors that affect the behavior of a structured soil, because looser soil skeleton structures can be considered to be formed by bonding effects. From a behavioral point of view, the macroscopic effect of such bonding reflects an overall increase of stiffness in much the same way as an increase in the over consolidation ratio and/or density. Therefore, the global bonding effect can be mathematically simulated by means of an “imaginary” increase of density, here denoted by the Greek letter  $\omega$ , despite the fact that the real structured soil may exist in looser states than a non-structured soil.

Figure 7 gives a zoom in part of region I of Fig. 6, showing the total change (finite increment) of void ratio when the stress condition moves from the initial state I ( $\sigma = \sigma_0$ ) to the current state P ( $\sigma = \sigma$ ) in the same way as

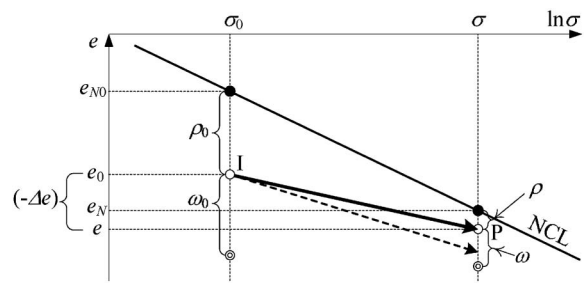


Fig. 7. Change of void ratio in a structured clay

those in Figs. 1 and 4. Here,  $e_0$  and  $e$  are the initial and current void ratios of the structured soil, and  $e_{N0}$  and  $e_N$  are the corresponding void ratios on the normally consolidated line, as described earlier. The lower arrow with a broken line represents the same change of void ratio as that in Fig. 4 for the over consolidated unstructured soil. It can be understood that structured soil is stiffer than a non-structured over consolidated soil, even if the initial state variable  $\rho_0$  is the same. Then, the change in void ratio for the structured soil indicated by the arrow with solid line is smaller than that for a non-structured over consolidated soil (arrow with broken line). Such an increase in stiffness will be expressed by introducing an imaginary density  $\omega$  which represents the effect of the bonding, in addition to the real density  $\rho$ . Here,  $\omega_0$  is the initial value of  $\omega$ .

Despite the fact that the structured soil shows a stiffer behavior up to certain stress level, the total change in the void ratio is computed in exactly the same way as developed for the unstructured soil and formulated in Eqs. (12) to (15). The main difference resides in the evolution law of the real density  $\rho$ , which is also capable of assuming negative values, as illustrated in Fig. 8, depending on the magnitude of the bonding effects represented by the imaginary density  $\omega$ . The solid line in Fig. 8 shows the relation between  $F$  and  $(H + \rho_0)$  for a structured soil. When the degradation of the bonding effect  $\omega$  is faster with the development of plastic deformation, the solid line monotonically approaches the broken line ( $F = H$ ) of the normally consolidated (NC) soil in the same way as that for the over consolidated soil shown in Fig. 5 (see diagram (a)). On the other hand, when the degradation of  $\omega$  is not so fast, the solid line reaches the broken line before complete debonding ( $\omega = 0$ ), so that the solid line enters in the region of  $\rho < 0$ . If it is assumed that negative  $\rho$  in effect decreases the stiffness contrary to positive  $\rho$ , the solid line finally approaches the broken line from the region of  $\rho < 0$ .

It is necessary to account for the effect of bonding on the evolution rule of the density variable  $\rho$ . This should still be dependent on the development of plastic deformation for the structured soil, so that  $d\rho \propto d(-e)^p$ . Furthermore, it is supposed that the degree of degradation of  $\rho$  can be determined not only by the state variable  $\rho$  related to the real density but also by the state variable  $\omega$  related to the imaginary increase of density due to bonding. This

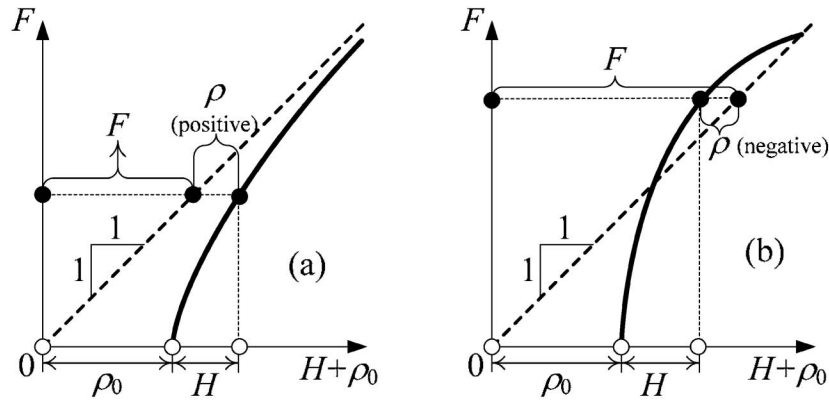


Fig. 8. Evolution of  $F$  and  $H$  in a structured soil  
(a) degradation of  $\omega$  is faster, (b) degradation of  $\omega$  is slower

will be introduced by an extra function  $Q(\omega)$  with an additive effect on the already defined function  $G(\rho)$ . As such, the evolution rule for  $\rho$  can be given in the following form:

$$d\rho = - \{ G(\rho) + Q(\omega) \} \cdot d(-e)^p \quad (19)$$

An additional evolution rule must also be introduced for the imaginary density. Here, this evolution rule of  $\omega$  is also given using the same function  $Q(\omega)$  as follows:

$$d\omega = - Q(\omega) \cdot d(-e)^p \quad (20)$$

It is also possible to define the evolution rule of  $\omega$  by another function that takes into account destructuring effects such as particle crashing due to increasing stress magnitude, decay of bonding due to chemical action and/or weathering and so on. Both functions  $G(\rho)$  and  $Q(\omega)$  must monotonically increase (or decrease) and satisfy the conditions,  $G(0)=0$  and  $Q(0)=0$ , so that the  $e$ - $\ln \sigma$  curve approaches the NCL when the soil becomes totally destructured ( $\omega = 0$ ) and normally consolidated ( $\rho = 0$ ). The domain of function  $G(\rho)$  can now assume positive or negative values of  $\rho$ , while  $\omega$  is always positive. This means that  $G(\rho)$  might be positive or negative while  $Q(\omega)$  is always positive. The simpler relations  $G(\rho)$  and  $Q(\omega)$  that satisfy the above restrictions are given by the linear increasing functions illustrated in Fig. 9. Here the slopes  $a$  and  $b$  of these lines are the material parameters which control the degradation rate of the state variables  $\rho$  and  $\omega$ , respectively.

Equations (15) and (19) give the increment of the plastic void ratio as

$$d(-e)^p = \frac{\lambda - \kappa}{1 + G(\rho) + Q(\omega)} \cdot \frac{d\sigma}{\sigma} \quad (21)$$

The increment of total void ratio is expressed as follow from Eqs. (9) and (21):

$$d(-e) = d(-e)^p + d(-e)^e = \left\{ \frac{\lambda - \kappa}{1 + G(\rho) + Q(\omega)} + \kappa \right\} \frac{d\sigma}{\sigma} \quad (22)$$

As shown in Eq. (21), positive values of  $\rho$  and  $\omega$  have the effects of increasing the stiffness of soils, because  $G(\rho)$

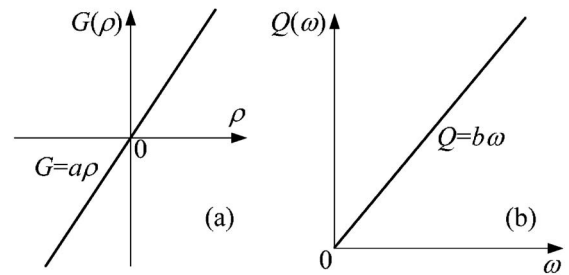


Fig. 9.  $G(\rho)$  and  $Q(\omega)$  given by linear functions

and  $Q(\omega)$  are positive in the case when  $\rho$  and  $\omega$  are positive.

A brief discussion is presented now to explain how the formulation of Eq. (21) can mathematically explain the conceptual behavior of structured soils under one-dimensional consolidation as depicted in Fig. 6. Assume an initial state with positive  $\rho_0$  and positive  $\omega_0$ . At the first stage ( $\rho > 0$  and  $\omega > 0$ ), the stiffness of the soil is much larger than that of normally consolidated (NC) soil, because of the positive values of  $G(\rho)$  and  $Q(\omega)$ . When the current void ratio becomes the same as that on the NCL ( $\rho = 0$ ), the stiffness of the soil is still larger than that of a NC soil because  $\omega > 0$ . In this way, it is possible to model the behavior of a structured soil with a looser but stiffer state than that on the NCL. In this stage ( $\rho < 0$  and  $\omega > 0$ ), the effect of increasing stiffness due to the positive value of  $\omega$  is larger than the effect of decreasing stiffness due to the negative value of  $\rho$ . After this stage the effect of  $\omega$  becomes smaller with the development of plastic deformation. On the other hand, the effect of  $\rho$  to decrease the stiffness becomes prominent because of the negative value of  $\rho$ . Finally the void ratio approaches to that on the NCL, because both  $\rho$  and  $\omega$  converge to zero.

### PARAMETRIC ANALYSES AND MODEL VALIDATION

In order to check the validity of the present model, numerical simulations of one-dimensional compression tests are carried out. The expressions of  $G(\rho)$  and  $Q(\omega)$  are

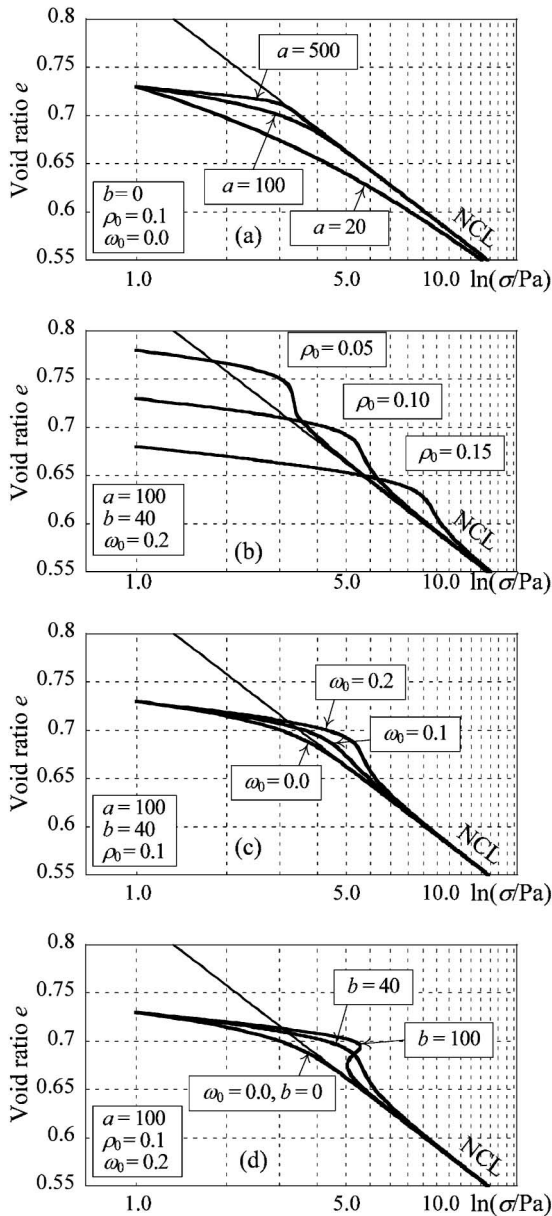


Fig. 10. Calculated results of clays with different  $\rho_0$ ,  $\omega_0$ ,  $a$  and  $b$  (where  $P_a$  = atmospheric pressure (98 kPa))

given by the simple linear functions of  $\rho$  and  $\omega$  in Fig. 9. Assuming Fujinomori clay which was used in the previous experimental verification of constitutive models (e.g., Nakai and Hinokio, 2004; Nakai, 2007), the following material parameters are employed in the numerical simulations: compression index  $\lambda = 0.104$ , swelling index  $\kappa = 0.010$  and void ratio on the NCL at  $\sigma = 98$  kPa (atmospheric pressure)  $N = 0.83$ .

Figure 10(a) shows the calculated  $e$ - $\log \sigma$  relation of the one-dimensional compression of remolded over consolidated clays without bonding ( $\omega_0 = 0$ ) for which the initial void ratios are the same ( $e_0 = 0.73$ ), but the parameter  $a$  assumes different values ( $a = 20, 100$  and  $500$ ) to check the sensitivity of the stress-strain behavior with this property. Figure 10(b) shows the calculated  $e$ - $\log \sigma$  relation of the one-dimensional compression of structured

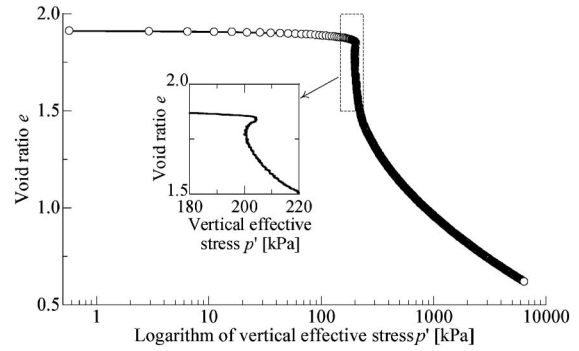


Fig. 11. Observed result of Luiseville clay with strain softening in constant strain rate one-dimensional consolidation test (plotted from data in Watabe et al., 2009)

clays using the same bonding effect ( $\omega_0 = 0.2$ ) and the different initial void ratios  $e_0 = 0.78, 0.73$  and  $0.68$  ( $\rho_0 = 0.05, 0.10$  and  $0.15$ ). Figure 10(c) shows the calculated results using the same initial void ratio  $e_0 = 0.73$  ( $\rho_0 = 0.1$ ) and different values of bonding parameters ( $\omega_0 = 0.0, 0.1$  and  $0.2$ ). Since the state variable related to density  $\rho (= e_N - e)$ , which is represented by the vertical distance between the current void ratio and the void ratio at the NCL, of the clay without bonding ( $\omega_0 = 0$ ) decreases monotonically, its void ratio converges to the NCL from below. The void ratio of the clay with bonding ( $\omega_0 > 0$ ) decreases less than that without bonding ( $\omega_0 = 0$ ) and enters the upper region of the NCL ( $\rho < 0$ ). After that, it converges to the NCL from the negative side of  $\rho$  with a sharp reduction of bulk stiffness. In these figures, the parameters ( $a$  and  $b$ ), which represent the degradation rate of  $\rho$  and  $\omega$ , are fixed. It can be seen from these figures that it is possible to describe the deformation of structured clays only by considering the effects of density and bonding and their evolution rules. Furthermore, Figure 10(d) shows the results in which the initial void ratio and the initial bonding are the same, but the parameter  $b$  assumes different values ( $b = 0, 40$  and  $100$ ). It can be seen that the results with larger value of  $b$  ( $= 100$ ) describe void ratio-stress relation with strain softening. Figure 11 shows the results of a constant strain rate consolidation test on Luiseville clay in Canada, which was carried out by Watabe et al. (2009). It can be seen from this figure that this natural clay shows strain softening behavior even in one-dimensional consolidation.

### ONE-DIMENSIONAL MODELING OF OTHER FEATURES BASED ON ADVANCED ELASTOPLASTICITY (STAGE III)

The model developed so far, up to stage II, can account for the important influences of density and bonding on the behavior of real soils. These effects, by means of their evolution laws, are dependent on the development of plastic strains. There are, however, many other relevant features, such as time, temperature and suction related phenomena, that affect the behavior of soils and that are not dependent on plastic deformation. This section

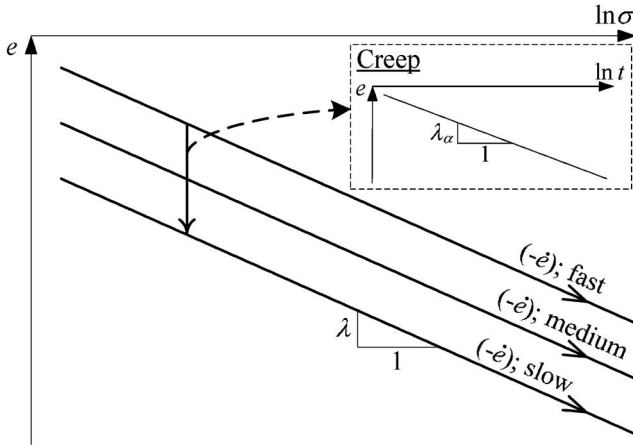


Fig. 12. Time dependent behavior of a normally consolidated clay

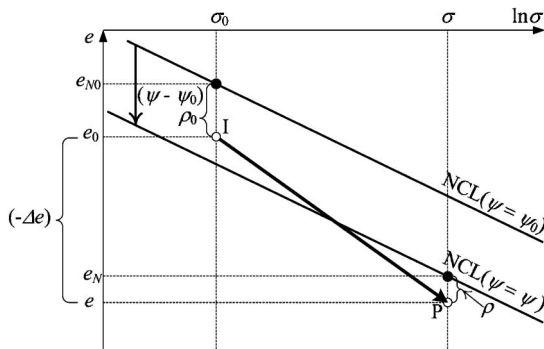


Fig. 13. Change of void ratio in an over consolidated clay and structured clay with some soil features such as time dependent behavior

presents a general framework in which these and other effects can be incorporated into an advanced model in a simple and unified manner.

For instance, Fig. 12 shows a schematic of the time-dependent behavior of a normally consolidated clay in the one-dimensional condition. It is well known that the normally consolidated line (NCL) shifts due to the strain rate (rate of void ratio change), and the void ratio ( $e$ ) changes linearly against time in a logarithmic scale ( $\ln t$ ) under the constant effective vertical stress (creep condition). In addition, experimental results show that the NCL (and/or the critical state line in a multi-dimensional state) also change depending on temperature, suction (saturation), etc. In order to model these features, a state variable, here generically denoted by  $\psi$ , will be introduced in this paper. This variable is independent of the plastic strains and will be controlled by a function of the strain rate (rate of void ratio change), temperature, suction (degree of saturation) and any other feature which shifts the position of the NCL, as shown in Fig. 13. Here,  $\psi_0$  is the initial value of  $\psi$ , and the points I and P indicate the initial ( $\sigma = \sigma_0$  and  $e = e_0$ ) and the current states ( $\sigma = \sigma$  and  $e = e$ ), respectively, in the same way as in Figs. 4 and 7. By referring to this figure, the plastic change of the void ratio  $(-\Delta e)^p$  for soil in which the above features should be considered is expressed as:

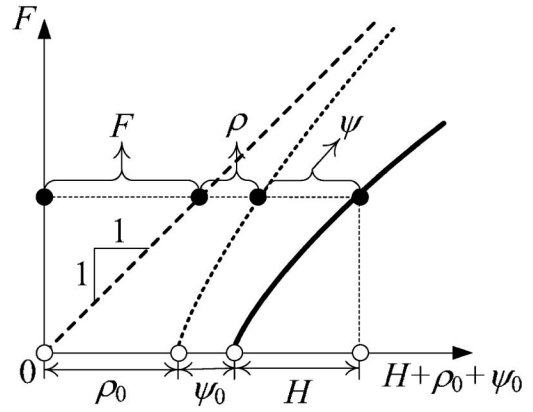


Fig. 14. Explanation of  $F$  and  $H$  in a clay with some features such as time dependent behavior

$$\begin{aligned}
 (-\Delta e)^p &= (-\Delta e) - (-\Delta e)^e \\
 &= \{(e_{N0} - e_N) - (\rho_0 - \rho)\} - (-\Delta e)^e \\
 &= \left\{ \lambda \ln \frac{\sigma}{\sigma_0} + (\psi - \psi_0) - (\rho_0 - \rho) \right\} - \kappa \ln \frac{\sigma}{\sigma_0} \\
 &= (\lambda - \kappa) \ln \frac{\sigma}{\sigma_0} - (\rho_0 - \rho) - (\psi_0 - \psi) \quad (23)
 \end{aligned}$$

Therefore, the following equation holds between  $F$  and  $H$ :

$$F + \rho + \psi = H + \rho_0 + \psi_0$$

or

$$f = F - \{H + (\rho_0 - \rho) + (\psi_0 - \psi)\} = 0 \quad (24)$$

Figure 14 shows Eq. (24) graphically as the relation between  $F$  and  $(H + \rho_0 + \psi_0)$ , in which the state variable  $\psi$  is assumed to be independent of the plastic deformation. Although  $\rho$  finally becomes zero with increasing plastic strain,  $\psi$  does not converge to zero but to some value depending on the current strain rate, temperature, suction and/or other features. Therefore, the solid line does not necessarily approach the broken straight line ( $F = H$ ), but becomes parallel to it. The following equation is obtained from Eq. (24) and consistency condition ( $df = 0$ ):

$$\begin{aligned}
 df &= dF - \{dH - d\rho - d\psi\} \\
 &= (\lambda - \kappa) \frac{d\sigma}{\sigma} - \{d(-e)^p - d\rho - d\psi\} = 0 \quad (25)
 \end{aligned}$$

Substituting  $d\rho$  with plastic deformation in Eq. (19) into Eq. (25), the increment of plastic void ratio can be obtained as:

$$d(-e)^p = \frac{(\lambda - \kappa) \frac{d\sigma}{\sigma} + d\psi}{1 + G(\rho) + Q(\omega)} \quad (26)$$

The increment of total void ratio is expressed as follows from Eqs. (9) and (26):

$$\begin{aligned}
 d(-e) &= d(-e)^p + d(-e)^e \\
 &= \left\{ \frac{\lambda - \kappa}{1 + G(\rho) + Q(\omega)} + \kappa \right\} \frac{d\sigma}{\sigma} + \frac{d\psi}{1 + G(\rho) + Q(\omega)} \quad (27)
 \end{aligned}$$

Here, the state variable  $\psi$  is a function of the rate of plastic void ratio change  $(-\dot{e})^p$  (or time  $t$ ), temperature  $T$ ,

suction  $s$  (or degree of saturation  $S_r$ ) or others, so that its increment  $d\psi$  is given in such forms as  $d\psi = (\partial\psi/\partial t)dt$ ,  $(\partial\psi/\partial T)dT$ ,  $(\partial\psi/\partial s)ds$ ,  $(\partial\psi/\partial S_r)dS_r$ , or others. Furthermore, if the model is formulated considering multiple features, different state variables  $\omega_a$ ,  $\omega_b$ ,  $\dots$  should be considered instead of a single  $\omega$ . Besides,  $\psi$  and  $\psi_0$  should be defined by the summation of the corresponding factors in a such a way that  $\psi = \psi_a + \psi_b + \dots$  and  $\psi_0 = \psi_{a0} + \psi_{b0} + \dots$ . Then, the evolution rules of  $\rho$  and the increment of  $\psi$  ( $d\rho$  and  $d\psi$  in Eq. (25)) are given as follows:

$$d\rho = -\{G(\rho) + Q_a(\omega_a) + Q_b(\omega_b) + \dots\} \cdot d(-e)^p \quad (28)$$

$$d\psi = d\psi_a + d\psi_b + \dots \quad (29)$$

Therefore, for considering multiple features, the increment of total void ratio is given by

$$d(-e) = \left\{ \frac{\lambda - \kappa}{1 + G(\rho) + Q_a(\omega_a) + Q_b(\omega_b) + \dots} + \kappa \right\} \frac{d\sigma}{\sigma} + \frac{d\psi_a + d\psi_b + \dots}{1 + G(\rho) + Q_a(\omega_a) + Q_b(\omega_b) + \dots} \quad (30)$$

The meaning of the state variables ( $\rho$ ,  $\omega$  and  $\psi$ ) in the proposed modeling are summarized as follows:

$\rho$ : State variable representing the density, which is defined by the difference between the current void ratio and the void ratio on the current NCL at the same stress level.

$\omega$ : State variable considering the effect that is degraded with the development of plastic deformation, such as the bonding effect in structured soil. The effect is represented by the imaginary increase in density.

$\psi$ : State variable describing the soil features, such as the time-dependent behavior, temperature-dependent behavior, and unsaturated soil behavior. This variable is not related with the development of plastic deformation. The features are considered by shifting the normally consolidated line (NCL) depending on the value of this state variable.

In order to obtain the stress-strain relation using the present model, it is necessary to determine the state variable  $\rho$  at every calculation step. Since the increment of total void ratio  $d(-e)$  is obtained from Eq. (27), the void ratio  $e_{(i)}$  at the current ( $i$ )<sup>th</sup> step can be updated from the void ratio  $e_{(i-1)}$  in the previous ( $i-1$ )<sup>th</sup> step and the increment  $d(-e)$ .

$$e_{(i)} = e_{(i-1)} - d(-e) \quad (31)$$

Then, the value of the state variable  $\rho$  at the current state can be calculated as the difference between the current void ratio  $e_{(i)}$  and the void ratio on the normally consolidated line (NCL at  $\psi = \psi$ ) at the current stress ( $\sigma = \sigma$ ).

The loading conditions of the present advanced models through stages I to III are presented as follows by assuming no occurrence of the plastic volume expansion:

$$\begin{cases} d(-e)^p \neq 0: & \text{if } d(-e)^p > 0 \\ d(-e)^p = 0: & \text{otherwise} \end{cases} \quad (32)$$

The loading condition using the increment of total void ratio  $d(-e)$  and the explicit expression of the incremental stress-stress relation are shown in APPENDIX I.

## APPLICATION OF THE ADVANCED MODEL (STAGE III) TO TIME-DEPENDENT BEHAVIOR OF SOIL IN ONE-DIMENSIONAL CONDITION

In the previous sections, formulations of the advanced elastoplastic models from stage I to stage III were shown. A method to describe time-dependent behavior of soil using the idea of stage III will be described in this section.

Several time-dependent constitutive models for soils are found in the literature. Sekiguchi (1977) proposed a viscoplastic model with a non-stationary flow surface. In this model, the non-stationary flow surface is obtained from the ordinary differential equation in which a unique relation between stress, plastic volumetric strain and plastic strain rate holds. Then the viscoplastic strain rate is calculated assuming a flow rule on the flow surface. Nova (1982) also developed a viscoplastic model by extending an inviscid model using non-stationary flow surface theory. Another type of viscoplastic model is based on the over-stress viscoplastic theory by Perzyna (1963) (e.g., Adachi and Oka, 1982; Dafalias, 1982; Katona, 1984), in which the strain rate effects can be described by assuming a Bingham like body and utilizing the difference of sizes of the current static yield surface related to the current plastic strains and the dynamic yield surface related to the current real stress. Hashiguchi and Okayasu (2000) developed a time-dependent subloading surface model introducing a creep potential function. Zhang et al. (2005) developed a time-dependent model for heavily over consolidated clays and soft rocks, modifying the subloading  $t_{ij}$  model developed by Nakai and Hinokio (2004). A comprehensive report on the time dependent behaviors of soils and their modeling has been written by Sekiguchi (1985).

In this section, a simple method to model time-dependent characteristics in normally consolidated soils, over consolidated soils and structured soils, such as naturally deposited clays, is presented which does not use the usual viscoplastic theories but refers to the above-mentioned formulations of advanced elastoplastic modeling (stage III).

Figure 15 shows a well-known creep behavior ( $e$ - $\ln t$  relation) for normally consolidated clays under constant stress. The void ratio at time  $t_0$  is  $e_0$ , and at time  $t$  it is  $e$ . Here,  $\lambda_\alpha$  is the coefficient of secondary consolidation. In this interval, only irreversible plastic change in the void ratio occurs, because the stress level is fixed.

Figure 16 shows the changes of the NCL and void ratio for the change of plastic strain rate (rate of plastic void ratio change) from  $(-\dot{e})_0^p$  to  $(-\dot{e})^p$  when the stress condition moves from the initial state I ( $\sigma = \sigma_0$ ) to the current state P ( $\sigma = \sigma$ ) in the normal consolidation condition. This change can be interpreted as a superposition of two effects: (a) the time dependent effect from point I to J, as depicted in Fig. 15, and (b) the stress change effect from point J to P, along the NCL which was shifted due to the time effects. Here,  $e_0$  and  $e$  are the initial and current void ratios on the normal consolidation line (NCL) at  $\psi = \psi_0$  and  $\psi = \psi$ , respectively, and  $\psi$  is a state variable which

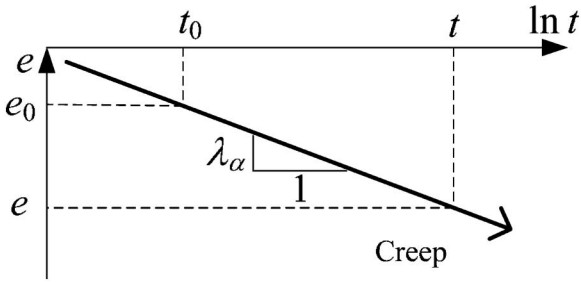


Fig. 15. Creep characteristics of a normally consolidated clay

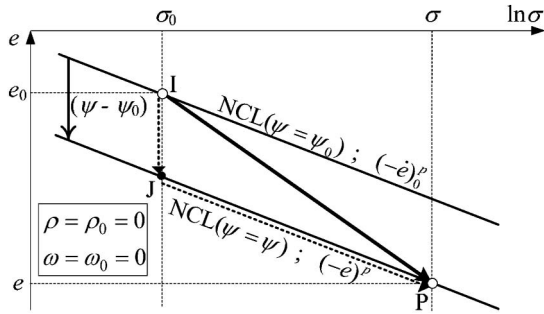


Fig. 16. Change in position of NCL and void ratio due to change in stress and strain rate for a normally consolidated clay

changes the position of the NCL upward and downward and is responsible for the time effect described earlier. The movement of the NCL ( $\psi - \psi_0$ ) can be obtained from Figs. 15 and 16 as

$$\psi - \psi_0 = \lambda_\alpha \ln \frac{t}{t_0} = \lambda_\alpha \ln t - \lambda_\alpha \ln t_0 \quad (33)$$

This equation can be rewritten using the plastic void ratio change instead of the elapsed time  $t$  as follows:

$$\psi - \psi_0 = \lambda_\alpha \ln \frac{(-\dot{e})_0^p}{(-\dot{e})^p} = \{-\lambda_\alpha \ln (-\dot{e})^p\} - \{-\lambda_\alpha \ln (-\dot{e})_0^p\} \quad (34)$$

To obtain the above equation, the following relation during creep deformation in normally consolidated soil was used:

$$(-\dot{e})^p = \frac{d(-\Delta e)^p}{dt} = \frac{d\left(\lambda_\alpha \ln \frac{t}{t_0}\right)}{dt} = \lambda_\alpha \frac{1}{t} \quad (35)$$

Therefore,  $\psi$  and  $\psi_0$ , which represent the positions of initial and current NCL, are determined as follows using the rate of plastic void ratio change:

$$\begin{cases} \psi = -\lambda_\alpha \ln (-\dot{e})^p \\ \psi_0 = -\lambda_\alpha \ln (-\dot{e})_0^p \end{cases} \quad (36)$$

From Eqs. (33) and (35), the increment  $d\psi$  is expressed as

$$d\psi = \frac{\partial \psi}{\partial t} dt = \lambda_\alpha \frac{1}{t} dt = (-\dot{e})^p dt \quad (37)$$

Equations (36) and (37) imply that the position of NCL ( $\psi$ ) and its increment ( $d\psi$ ) can be expressed by the rate of

plastic void ratio change instead of the elapsed time. It is assumed that Eqs. (36) and (37) hold not only for normally consolidated soils but also for over consolidated soils and naturally deposited soils. Substituting Eq. (37) into Eq. (26), the increment of the plastic void ratio can be obtained as:

$$\begin{aligned} d(-e)^p &= \frac{(\lambda - \kappa) \frac{1}{\sigma} d\sigma + (-\dot{e})^p \cdot dt}{1 + G(\rho) + Q(\omega)} \\ &\cong \frac{(\lambda - \kappa) \frac{1}{\sigma} d\sigma + (-\dot{e})^{p*} \cdot dt}{1 + G(\rho) + Q(\omega)} \end{aligned} \quad (38)$$

Here,  $(-\dot{e})^{p*}$  denotes the rate of the plastic void ratio change at the step immediately before the current calculation step. Finally, the total increment of void ratio is given in the following equation:

$$\begin{aligned} d(-e) &= d(-e)^p + d(-e)^e = \left( \frac{\lambda - \kappa}{1 + G(\rho) + Q(\omega)} + \kappa \right) \frac{d\sigma}{\sigma} \\ &\quad + \frac{(-\dot{e})^{p*}}{1 + G(\rho) + Q(\omega)} dt \end{aligned} \quad (39)$$

In order to simplify the numerical calculations, the known rate  $(-\dot{e})^{p*}$  in the previous calculation step can be used instead of the current rate, as described in Eqs. (38) and (39). The error caused by using the previous known rate is negligible in the calculations since an incremental method with small steps is used in the non-linear analysis. As can be seen from Eq. (19), the void ratio approaches the condition satisfying  $G(\rho) + Q(\omega) = 0$ , regardless of the sign of  $\rho$ . Here,  $\rho$  represents the difference between the current real void ratio and the void ratio on the NCL, which shifts depending on the current rate  $(-\dot{e})^p$  as mentioned above. Therefore, even if some small error occurs due to the use of  $(-\dot{e})^{p*}$  in the numerical calculation, the error is automatically corrected in the next step by updating the rate with the calculated plastic change in void ratio at each time increment and reflecting it on the state variable  $\psi$ ; that is, the error caused in one calculation step is corrected in the next. The model requires only one additional parameter, which is the coefficient of secondary consolidation  $\lambda_\alpha$ , to account for the time effect. An interesting point of the present model is that the present model does not include time variable  $t$  and is formulated using the rate of void ratio change  $(-\dot{e})^p$  alone. If time  $t$  is used in a model, the results will depend on the way the origin of time is determined. Another characteristic of the proposed approach is that by only eliminating the term of the rate effect  $(-\dot{e})^{p*}$  in Eq. (39), or by setting  $\lambda_\alpha = 0$ , this model easily results in the elastoplastic model without a time effect.

The formulation of the time effect in the present model is based on experimental evidence which shows that there is a unique relation between stress, strain (void ratio) and strain rate (rate of void ratio change) under loading for normally consolidated clay, in the same way as assumed in Sekiguchi's model (Sekiguchi, 1977). This is called

'isotache'. Sekiguchi's model is formulated using a non-stationary flow surface obtained by solving this relation in the form of an ordinary differential equation between stress, plastic strain and plastic strain rate. On the other hand, the present model is formulated by defining the plastic strain rate (rate of plastic void ratio change) as a state variable and using the implicit idea of a subloading surface concept. The meaning of the present time-dependent model and the common points and differences between the present model and the non-stationary flow surface model proposed by Sekiguchi are described in APPENDIX II.

### SIMULATION OF TIME-DEPENDENT BEHAVIOR OF SOIL IN ONE-DIMENSIONAL CONDITION

The validity of the proposed time-dependent model is checked by simulations of one-dimensional compression behavior under constant strain rate for an infinitesimal soil element and by simulations of conventional oedometer tests with instantaneous loading of constant stress as a boundary value problem using one-dimensional soil-water coupled finite element analyses. The adopted parameters are the same as those of Fujinomori clay used in the previous section—i.e., compression index  $\lambda = 0.104$ , swelling index  $\kappa = 0.010$ , void ratio on the NCL at  $\sigma = 98$  kPa  $N = 0.83$ . The evolution rule for  $\rho$  is considered as a linear function,  $G(\rho) = a\rho$ , and the evolution rule for  $\omega$  is also considered as a linear function,  $Q(\omega) = b\omega$  as indicated in Fig. 9. The parameter for density and confining pressure  $a = 100$ , and the degradation parameter of bonding  $b = 40$ , unless otherwise stated. The initial value of  $\omega$  for the soil with bonding is  $\omega_0 = 0.2$ . The rate of the plastic void ratio change at reference state is  $(-\dot{e})_{\text{ref}}^p = 1.0 \times 10^{-7}/\text{min}$ . Here, the coefficient of secondary consolidation  $\lambda_\alpha$  is 0.003, unless otherwise stated. The values of material parameters of Fujinomori clay for time-dependent model are summarized in Table 1. Some of the methods used to determine the material parameters of the evolution rules of  $\rho$ ,  $\omega$  and the position

of NCL ( $\psi$ ) for a naturally deposited clay are presented as follows. The compression index  $\lambda$ , the swelling index  $\kappa$  and the coefficient of secondary consolidation  $\lambda_\alpha$  are derived from the loading and unloading  $e$ - $\ln \sigma$  relation and the  $e$ - $\ln t$  relation obtained from the usual oedometer tests on remolded and normally reconsolidated samples. The evolution rule of  $\rho$  can be determined by fitting the calculated  $e$ - $\ln \sigma$  relation of remolded and over consolidated sample to the observed one, referring to the sensitivity of the parameter  $a$  (e.g., Fig. 10(a)), because the bonding effect is considered to be zero in remolded reconsolidated samples. Then, the evolution rule of bonding ( $b$  and  $\omega_0$ ) is determined by fitting the calculated  $e$ - $\ln \sigma$  relation of the undisturbed naturally deposited clay to the observed one referring to the sensitivity of these parameters (e.g., Figs. 10(b) to (d)). The position of the NCL ( $\psi$ ) in the time-dependent model is determined from the rate  $(-\dot{e})^p$  and the coefficient of secondary consolidation  $\lambda_\alpha$  (see Eq. (36)). Here, it can be considered that although the material parameters, except for  $\omega_0$ , are independent of the initial conditions (void ratio, stress level and others),  $\omega_0$  depends on the degree of the initial natural cementation (bonding).

Figure 17 shows the simulated results of one-dimensional compression behavior of a normally consolidated clay for different strain rates, arranged in terms of the  $e$ - $\log \sigma$  relation. The initial rate of plastic void ratio change is the same as that at the reference state ( $(-\dot{e})_0^p = (-\dot{e})_{\text{ref}}^p = 1.0 \times 10^{-7}/\text{min}$ ). In the figure, the solid straight line (no creep) shows a simulated relation with no time effect. The simulated result by the time-dependent model with the constant rate of  $(-\dot{e})_0^p = (-\dot{e})_{\text{ref}}^p$  also coincides with the solid straight line. In this figure, the resistance to compression increases and the lines of constant strain rate become parallel to each other with increasing strain rate, which is in agreement with published experimental results (e.g., Bjerrum, 1967). It is also seen that when the strain rate changes at a certain point, the curve follows exactly the same path the new rate is supposed to follow. This is

Table 1. Values of material parameters for Fujinomori clay in time-dependent model

$\lambda$	0.104
$\kappa$	0.010
$N$ ( $e_N$ at $\sigma = 98$ kPa)	0.83
$a$	100
$b$	40 unless otherwise stated
$\omega_0$	0.0 (without bonding)
	0.2 (with bonding)
$\lambda_\alpha$	0.003 unless otherwise stated
$(-\dot{e})_{\text{ref}}^p$	$1 \times 10^{-7}/\text{min}$ .

N.B.  $N$  is the void ratio of NCL at  $(-\dot{e})^p = (-\dot{e})_{\text{ref}}^p$

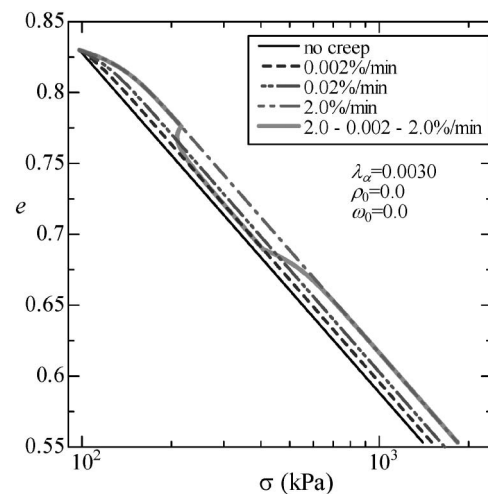


Fig. 17. Calculated  $e$ - $\log \sigma$  relations under constant strain rates for normally consolidated clays

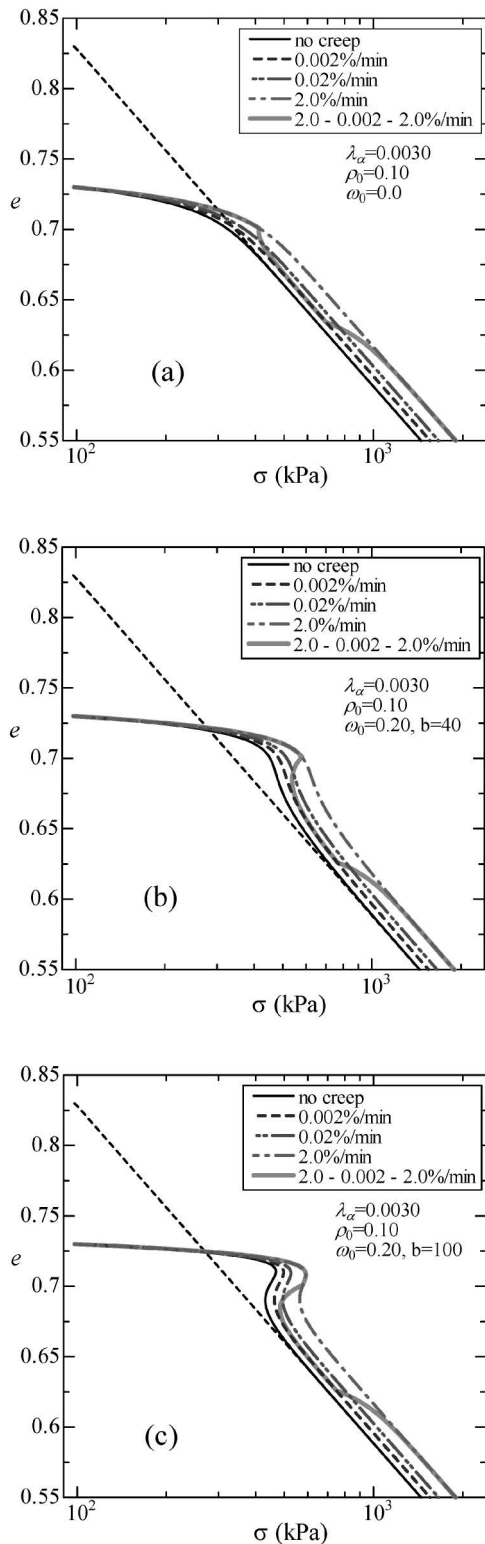


Fig. 18. Calculated  $e$ -log  $\sigma$  relations under constant strain rates for over consolidated and over consolidated-structured clays

valid for both increasing and decreasing the strain rates, and in the case where the strain rate is increased the simulation gradually reaches the target curve following the phenomenon of ‘isotache’. Therefore, it can be said that the present model can describe properly the strain rate effects of a non-structured normally consolidated clay ( $\omega_0$

$= 0$  and  $\rho_0 = 0$ ) under constant strain rate consolidation tests.

Figure 18(a) represents the calculated  $e$ -log  $\sigma$  relations for an over consolidated non-structured clay ( $\omega_0 = 0$  and  $\rho_0 \neq 0$ ) subjected to different strain rates. Here, at the initial stress condition ( $\sigma_0 = 98$  kPa), the void ratio is  $e_0 = 0.73$ , the rate of plastic void ratio change is the same as that at reference state ( $-\dot{e}_0^p = (-\dot{e})_{\text{ref}}^p = 1.0 \times 10^{-7}/\text{min}$ ), and the void ratio on the NCL at  $\sigma = 98$  kPa is  $e_{N0} = 0.83$ . Therefore, the initial value of density state variable is  $\rho_0 = 0.10$ . Figure 18(b) illustrates the results for an over consolidated-structured soil. Here, the initial void ratio and the initial rate of strain are the same as those of diagram (a). The initial value of the state variable reflecting the bonding effect is  $\omega_0 = 0.20$ , and the bonding degradation parameter is  $b = 40$ . In the figures, the dotted straight line denotes the normal consolidation line (NCL) for  $(-\dot{e})^p = (-\dot{e})_{\text{ref}}^p = 1.0 \times 10^{-7}/\text{min}$ . It can be observed that the strain rate dependency of the soil is less significant for over consolidated states compared to normally consolidated states. However, each  $e$ -log  $\sigma$  relation for over consolidated soils and structured soils finally approaches the line simulated for normally consolidated soil under the corresponding strain rate. Figure 18(c) shows the results of the over consolidated-structured soil for the same material parameters as illustrated in diagram (b), but using a different bonding degradation parameter ( $b = 100$ ). The results show both hardening and softening behaviors of soil for different strain rates. In these figures, the thick curves represent the results in which the strain rate decreases and increases again during loading in the same way as that in Fig. 17. The simulated results of the over consolidated clay and the structured clays also tend to the curve that corresponds to the new strain rates. The phenomenon of ‘isotache’ is simulated for over consolidated and structured soils, in the same way as observed for the normally consolidated soil. This phenomenon was observed by Leroueil et al. (1985) in their one-dimensional compression tests with natural clay (Batiscan clay). In diagrams (a) to (c) in Fig. 18, each solid curve designated as ‘no creep’ is the same as the corresponding curve without time effect in Fig. 10(d). It is also seen that the ‘preconsolidation’ stress (effective consolidation yield stress)  $p_c$  increases with increasing strain rates, particularly in structured clays. These simulations in Figs. 18 describe well the strain rate effects in one-dimensional compression for over consolidated clay and structured clay reported in the literature (e.g., Leroueil et al., 1985; Tanaka et al., 2006; Watabe et al., 2008).

Figure 19 shows the simulated results of the one-dimensional compression behavior under constant strain rate tests including some stress relaxation periods on a structured soil. Here, the initial condition is the same as that in Fig. 18(b)—i.e.,  $\rho_0 = 0.10$ ,  $\omega_0 = 0.20$  and  $b = 40$ . Diagram (a) shows the results arranged in terms of the relation between void ratio and stress in log scale for different strain rates, and diagram (b) shows the reduction of stress  $\sigma$  during stress relaxation period. The stress in diagram (b) is normalized by the maximum stress value  $\sigma_{\text{max}}$

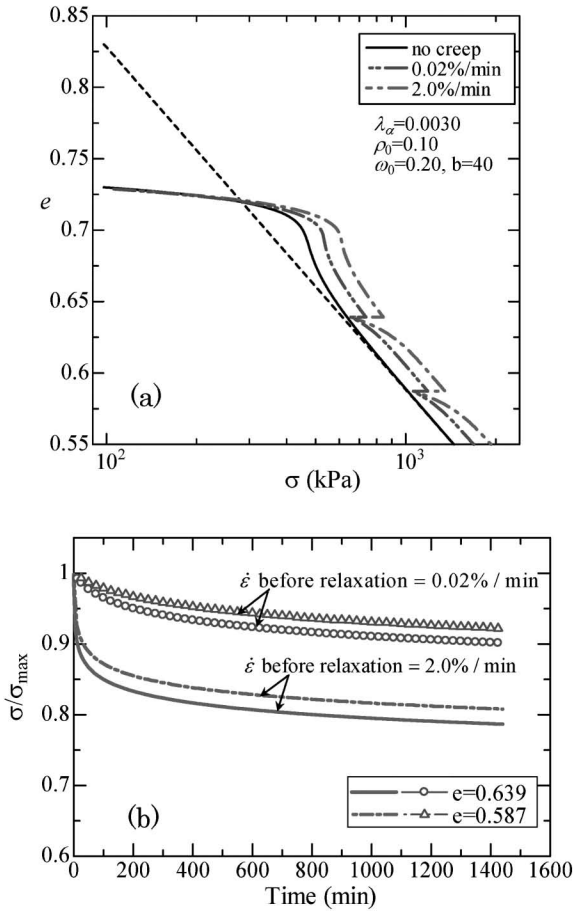


**Fig. 19. Calculated consolidation behavior under constant strain rate including some stress relaxation periods for structured clays**  
 (a) vertical stress in log scale vs. void ratio  
 (b) reduction of stress during stress relaxation period

imposed at the start of the corresponding relaxation.

Tanaka et al. (2006) carried out one-dimensional constant strain rate consolidation tests including some stress relaxation periods for different strain rates on undisturbed Osaka Pleistocene clay (Ma12 layer). Figure 20 shows the observed results of their tests, arranged in the same form as those in Figs. 19(a) and (b). It can be seen from these figures that the present model simulates well the observed features of the naturally deposited clay, — i.e., the yield stress becomes larger with increasing strain rate, the shape of  $e$ -log  $\sigma$  relation (or  $\varepsilon$ -log  $\sigma$  relation) is almost independent of the strain rate, and the normalized relaxation stress  $\sigma/\sigma_{max}$  shows more or less the same tendency if the strain rates at the start of the relaxation are the same.

One-dimensional soil-water coupled finite element analyses of oedometer tests with instantaneous loading of constant vertical stress were carried out to investigate the consolidation characteristics of clays. In the simulations of oedometer tests, the height  $H$  of the sample was divided into elements of 0.1 cm thick, as shown in Fig. 21, and drainage was allowed at the top boundary of the sample while the bottom boundary was considered undrained. In order to make the coefficient of consolidation  $c_v$  constant

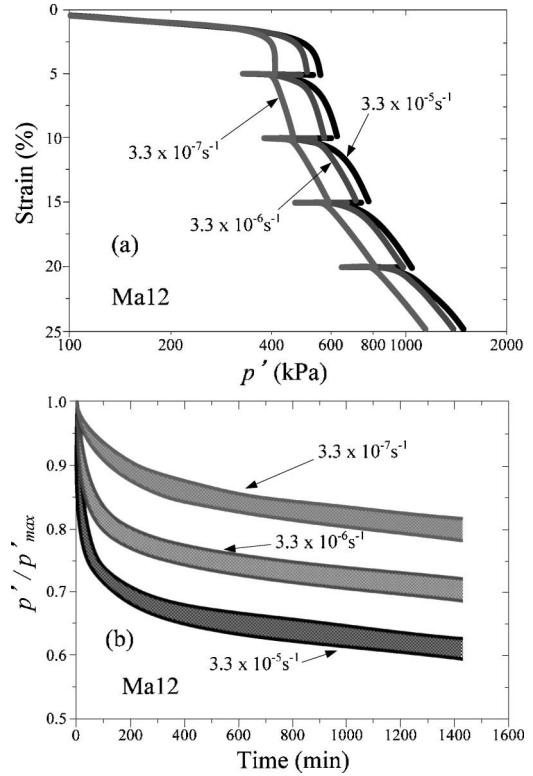


**Fig. 20. Observed results of constant strain rate consolidation tests including some stress relaxation periods on Osaka pleistocene clay (replotted from data in Tanaka et al., 2006)**  
 (a) vertical stress in log scale vs. strain  
 (b) reduction of stress during stress relaxation period

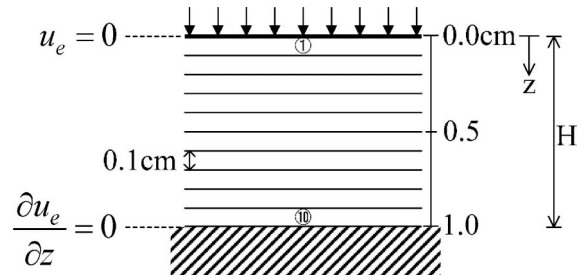


**Fig. 21. Finite element mesh and boundary condition in the one-dimensional consolidation simulations ( $H = 1$  cm)**

during normal consolidation, regardless of the stiffness of the soil, the following relationship between the coefficient of permeability  $k$  and the current void ratio  $e$  was used in these simulations;

$$k = k_0 \cdot \exp\left(\frac{e - e_{N0}}{\lambda_k}\right) \quad (40)$$

where,  $e_{N0} = 0.83$ ,  $k_0 = 1.0 \times 10^{-5}$  cm/min and  $\lambda_k = 0.104$ , which is the same as the compression index  $\lambda$ .

Figure 22 shows the computed  $e$ -log  $t$  simulations of conventional oedometer tests for a normally consolidated clay, where the initial stress was  $\sigma_0 = 98$  kPa, the initial rate of void ratio change was  $(-\dot{e})_0^p = 1.0 \times 10^{-7}$ /min and the instantaneous increment of stress  $\Delta\sigma = 98$  kPa was applied. After applying the stress increment, the consoli-

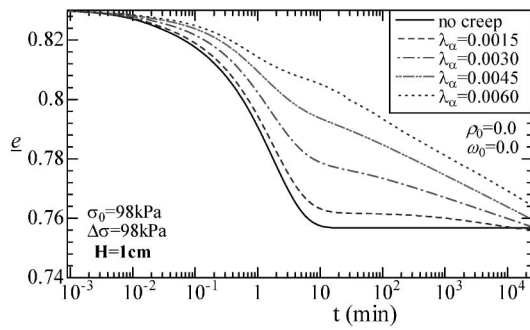


Fig. 22. Simulation of oedometer tests on a normally consolidated clay for different coefficients of secondary consolidation

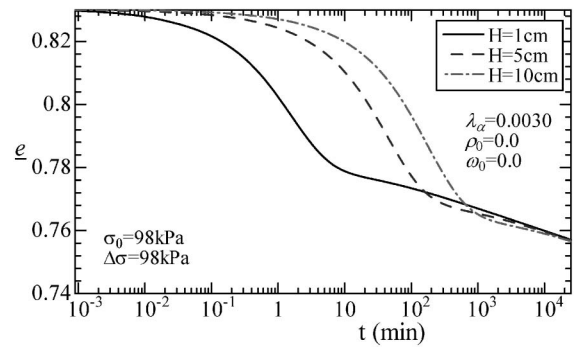


Fig. 23. Simulation of oedometer tests on normally consolidated clays for different heights of sample

dation behavior of the soil was investigated for different values of the coefficient of secondary consolidation ( $\lambda_\alpha$ ). The vertical axis ( $e$ ) represents the average void ratio of the soil mass. Here,  $H$  is the sample height, which represents the maximum drainage distance in the sample. The solid curve (no creep) represents the results where the effect of secondary consolidation is not considered. A delay in consolidation occurs when the time effect is considered, which shows the creep behavior of the soil. With the increase of the value of  $\lambda_\alpha$ , the delay in consolidation becomes more remarkable. In the cases where the time effect is not much prominent, the curves of void ratio (settlement) versus the logarithm of time have the shape of reverse ‘s’ during the dissipation process of pore water pressure, as is commonly seen in the literature. During secondary consolidation, the slopes of the curves are the same as the coefficients of secondary consolidation ( $\lambda_\alpha$ ) which are employed in the simulations.

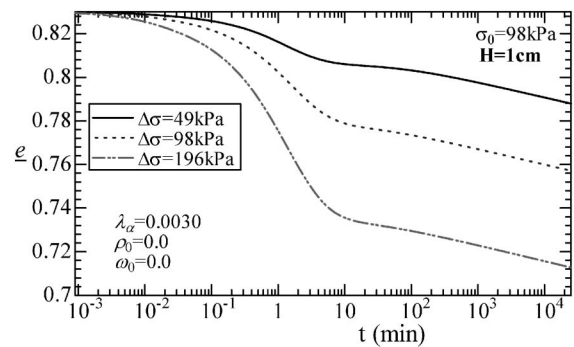


Fig. 24. Simulation of oedometer tests on normally consolidated clays for different stress increments

Figure 23 represents the computed  $e$ - $\log t$  relation for the normally consolidated clay with different heights of the sample ( $H = 1$  cm, 5 cm and 10 cm). The initial condition of each sample was  $\sigma_0 = 98$  kPa,  $(-e)_0^0 = 1.0 \times 10^{-7}$  /min, and the increment of the stress was  $\Delta\sigma = 98$  kPa. This figure describes the well-known effects of sample height (e.g., Aboshi, 1973; Ladd et al., 1977). Some time after the load is applied, the consolidation curves for different sample heights converge to a single curve. This tendency of  $e$ - $\log t$  curves under different sample heights corresponds to the curve referred to as ‘‘Type B’’ by Ladd et al. (1977). Figure 24 illustrates the computed  $e$ - $\log t$  relation for a normally consolidated clay with different stress increments ( $\Delta\sigma$ ). Here, the height of the sample was 1 cm and the coefficient of secondary consolidation ( $\lambda_\alpha$ ) was 0.003 in the same way as those in Fig. 23. The final slope of each curve after the dissipation of the excess pore water pressure is independent of the increment of stress ( $\Delta\sigma$ ), and is the same as the coefficient of secondary consolidation. The tendency of the computed results in Fig. 24 has good qualitative correspondence with published experimental results (e.g., Leonards and Girault, 1961; Oshima et al., 2002). Figure 25 shows the observed  $\varepsilon$ - $\log t$  relation of oedometer tests on remolded normally consolidated Osaka Nanko clay under different stress increments (Oshima et al., 2002).

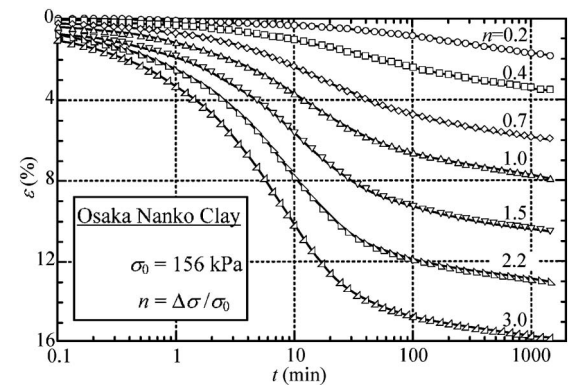


Fig. 25. Observed results of oedometer tests on remolded normally consolidated Osaka Nanko clay for different stress increments (Oshima et al., 2002)

Figure 26 shows the computed  $e$ - $\log t$  response for an over consolidated clay with different values of the coefficient of secondary consolidation ( $\lambda_\alpha$ ). Here, the over consolidation ratio was 1.70 ( $\rho_0 = 0.05$ ). The other conditions were the same as those for the normally consolidated clay in Fig. 22. After the excess pore water pressure dissipates, the slope of the curve for the over consolidated clay becomes much flatter than that of the normally consolidated clay, as is clear in Fig. 22, but becomes steeper again over time. Figure 27 shows the observed result of oedometer tests on over consolidated Hiroshima clay per-

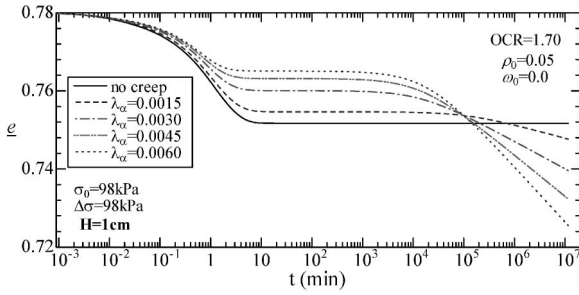


Fig. 26. Simulation of oedometer tests on an over consolidated clay for different coefficients of secondary consolidation

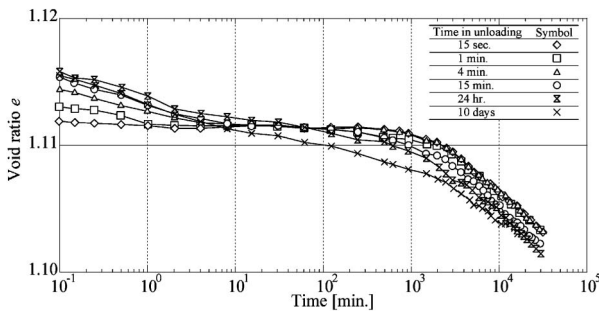


Fig. 27. Experimental results of oedometer tests on over consolidated clays (Yoshikuni et al., 1990)

formed by Yoshikuni et al. (1990). Here, the over consolidated clay, which was obtained by unloading the vertical stress from  $\sigma = 314$  kPa to  $\sigma = 157$  kPa on a remolded normally consolidated clay, is reloaded instantaneously to  $\sigma = 294$  kPa. ‘Time in unloading’ in the legend denotes the time during unloaded state at  $\sigma = 157$  kPa. The results of the simulation in Fig. 26 describe well the observed feature of the over consolidated clay in Fig. 27.

A sudden increase and delay in settlement after excess pore water pressure has almost dissipated has been observed in oedometer tests on natural clays (e.g., Leroueil, et al., 1985). Asaoka et al. (2000b) simulated such behavior with a soil-water coupled finite element analysis using an inviscid model for structured soils and stated that the strain softening characteristics with volume contraction for highly structured clay, and the migration of pore water in the clay due to Darcy’s law caused the delay of compression. Figure 28 shows the computed  $e$ - $\log t$  response of non-structured and structured clays in normally consolidated and over consolidated states. Diagram (a) shows the results under a small stress increment (the ratio of stress increment to initial stress:  $\Delta\sigma/\sigma_0 = 1$ ), and diagram (b) shows the results under large stress increment ( $\Delta\sigma/\sigma_0 = 4$ ). Here, the thin curves indicate the results of a non-structured clay ( $\omega_0 = 0.0$ ), and the thick curves show the results of a structured clay ( $\omega_0 = 0.2$ ). It is seen that although the behavior of the normally consolidated structured clay (OCR = 1.0) is different from that of the normally consolidated non-structured clay under small stress increment, not much difference is noted between them under large stress increment. On the other

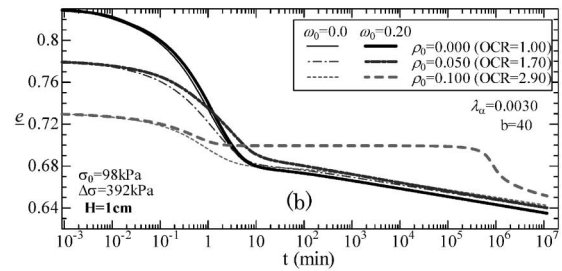
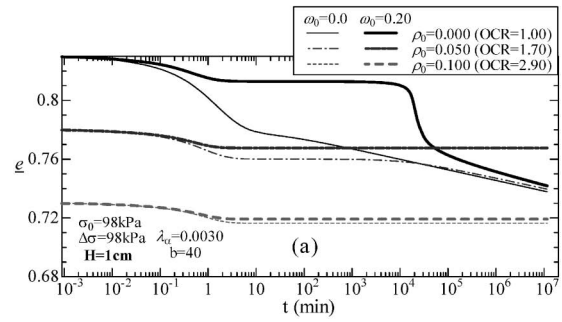


Fig. 28. Simulation of oedometer tests on non-structured and structured clays for different initial void ratios (a)  $\Delta\sigma/\sigma_0 = 1$ , (b)  $\Delta\sigma/\sigma_0 = 4$

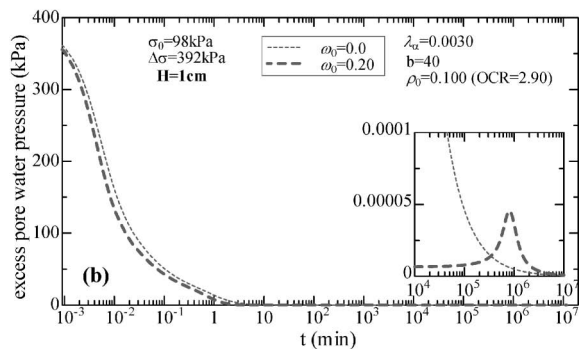
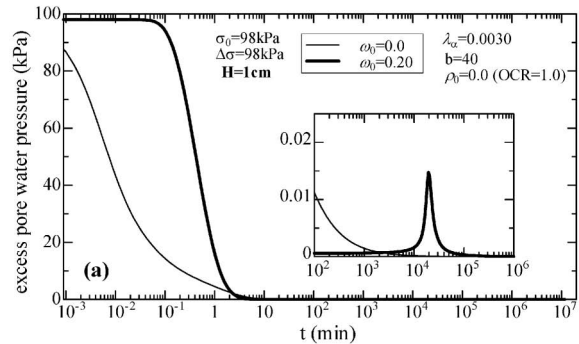


Fig. 29. Computed variations of excess pore water pressure with time at element 10 in oedometer tests on non-structured and structured clays for different initial void ratios (a)  $\Delta\sigma/\sigma_0 = 1$  and  $\rho_0 = 0.00$  (OCR = 1.0), (b)  $\Delta\sigma/\sigma_0 = 4$  and  $\rho_0 = 0.10$  (OCR = 2.9)

hand, the behavior of over consolidated clays (OCR = 2.9) is highly influenced by the effect of the structure (bonding) not under small stress increments but under large stress increments. Figure 29 shows the computed

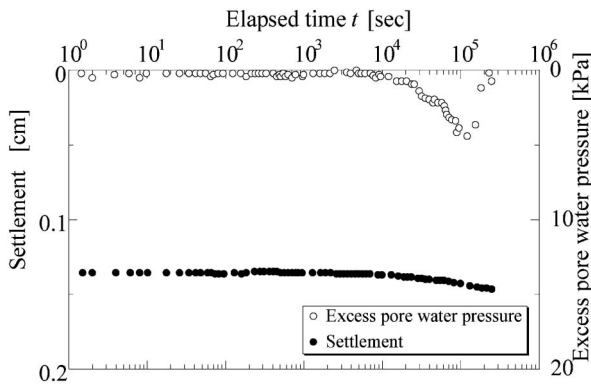


Fig. 30. Observed variations of settlement and excess pore water pressure with time in oedometer test on crushed mudstone pebbles (Kaneda, 1999)

variations of the excess pore water pressure with elapsed time at the element ⑩ in Fig. 21 for structured and non-structured clays. It can be seen from Figs. 28 and 29 that when delayed settlements occur for the structured clay, the pore water pressure, which has almost completely dissipated but has not reached zero, increases again and then decreases to zero. As described before, an over consolidated structured clay ( $\rho_0 = 0.1$ ,  $\omega_0 = 0.2$ ,  $b = 40$ ) may not exhibit strain softening behavior (see Fig. 18(b)). Figure 30 shows the observed variations of the settlement and the excess pore water pressure with time in an oedometer test ( $\sigma = 78$  kPa) on a saturated crushed mudstone, which is described in Kaneda (1999). It has been reported that the crushed mudstone behaves similarly to structured clays (Nakano et al., 1998). In the experiment, drainage is allowed only at the top of the specimen, and the pore water pressure is measured at the bottom of the specimen in the same way as the condition of the simulation in Fig. 21. The computed results in Figs. 28 and 29 describe well the features observed in oedometer tests on structured soil in Fig. 30—i.e., delayed settlement and delayed development of pore water pressure. Therefore, the delay of compression on saturated natural clay can mostly be attributed to the bonding effect and the time-dependent behavior of clay. According to the present results, it is presumed that when a large overburden load is applied on an over consolidated structured clayey ground, large delayed creep settlement may occur after excess pore water pressure is almost dissipated.

## CONCLUSIONS

After interpreting the one-dimensional behavior of normally consolidated soils under the framework of conventional elastoplastic theory, the following approaches to describe various features of one-dimensional soil behaviors for over consolidated and structured soils were formulated based on concepts of advanced elastoplasticity:

(1) Modeling in stage I: A simple method to describe the behavior of over consolidated soils was presented by introducing one state variable ( $\rho$ ) which is related to

density and assuming a monotonic evolution rule for this variable. This formulation is, in a sense, a one-dimensional interpretation of the subloading surface concept proposed by Hashiguchi (1980).

- (2) Modeling in stage II: Using not only the state variable ( $\rho$ ) but also another state variable ( $\omega$ ) which represents the effect of bonding and assuming a monotonic evolution rule in the same way as that of the state variable ( $\rho$ ), the behavior of structured soils, such as naturally deposited clays, was modeled.
- (3) Modeling in stage III: Since it is experimentally known that the  $e$ - $\ln \sigma$  normally consolidated line (NCL) shifts depending on the strain rate, temperature, suction (saturation) and other effects, another state variable ( $\psi$ ) which shifts the position of NCL was defined. Using this state variable together with  $\rho$  and  $\omega$ , a general method to take into consideration the time-dependent behavior, the temperature-dependent behavior or the behavior of unsaturated soil in the constitutive modeling was presented.
- (4) As an application of advanced modeling in stage III, a unique time-dependent model for normally consolidated soils, over consolidated soils and structured soils was developed. Time-dependent behavior was formulated without using previous viscoplastic theories, such as non-stationary flow surface and over stress concepts, but by introducing the state variable  $\psi$  and using the subloading surface concept.

The validity of the present models (stages I to III) was confirmed by the simulations of the one-dimensional tests on clays with different initial densities, bonding effects and strain rates. The models were also checked using soil-water coupled finite element analyses, and the computed results were shown to appropriately simulate many well-known consolidation behaviors reported in the literature, including secondary consolidation in oedometer tests for normally consolidated, over consolidated remolded and structured clays. These one-dimensional models can be easily extended to three-dimensional ones by introducing the  $t_{ij}$  concept (Nakai and Mihara, 1984). The formulation of three-dimensional models is shown in another paper (Nakai et al., 2011).

## ACKNOWLEDGMENTS

This study was supported financially in part by the Grant-in-Aid for Scientific Research (B-22360184, Teruo Nakai) from the Ministry of Education, Science and Culture of Japan.

## NOTATION

$a$ : material parameter to describe the influence of density and/or confining pressure

$b$ : material parameter to describe the influence of bonding

$e$ : void ratio

$e_N$ : void ratio on normally consolidation line (NCL)

$f=0$ : yield function

$k$ : coefficient of permeability  
 $t$ : time  
 $F$ : stress term in yield function ( $= (\lambda - \kappa) \ln (\sigma / \sigma_0)$ )  
 $G(\rho)$ : increasing function of  $\rho$  which satisfies  $G(0) = 0$   
 $H$ : plastic strain term in the yield function ( $= (-\Delta e)^p$ )  
 $N$ : void ratio of NCL at  $\sigma = 98$  kPa (at  $(-\dot{e})^p = (-\dot{e})_{ref}^p$  in case of time-dependent model)  
 $Q(\omega)$ : increasing function of  $\omega$  which satisfies  $Q(0) = 0$   
 $\varepsilon$ : strain  
 $\kappa$ : swelling index  
 $\lambda$ : compression index  
 $\lambda_k$ : coefficient for considering the influence of void ratio on permeability  
 $\lambda_a$ : coefficient of secondary consolidation  
 $\rho$ : state variable representing density—difference between current void ratio and void ratio on the NCL at same stress level  
 $\sigma$ : stress  
 $\omega$ : state variable considering bonding effect as an imaginary increase of density  
 $\psi$ : state variable for shifting the NCL on  $e$ - $\ln \sigma$  plane  
 superscript  $e$ : elastic component  
 superscript  $p$ : plastic component  
 subscript 0: initial value  
 subscript  $ref$ : value at reference state  
 overhead dot ( $\dot{\cdot}$ ): rate of quantities  
 prefix  $d$ : infinitesimal increment of quantities  
 prefix  $\Delta$ : finite change in quantities

## REFERENCES

- Aboshi, H. (1973): An experimental investigation on the similitude in the consolidation of a soft clay, including the secondary creep settlement, *Proc. of 8th International Conf. on Soil Mech. and Foundation Eng.*, Moscow, **4.3**, 88.
- Adachi, T. and Oka, F. (1982): Constitutive equation for normally consolidated clays based on elasto/viscoplasticity, *Soils and Foundations*, **22**(4), 57–70.
- Asaoka, A., Nakano, M. and Noda, T. (2000a): Superloading yield surface concept for highly structured soil behaviour, *Soils and Foundations*, **40**(2), 99–110.
- Asaoka, A., Nakano, M., Noda, T. and Kaneda, K. (2000b): Delayed compression/consolidation of natural clay due to degradation of soil structure, *Soils and Foundations*, **40**(3), 75–85.
- Asaoka, A., Noda, T., Yamada, E., Kaneda, K. and Nakano, M. (2002): An elasto-plastic description of two distinct volume change mechanism of soils, *Soils and Foundations*, **42**(5), 47–57.
- Asaoka, A. (2003): Consolidation of clay and compaction of sand—an elastoplastic description, *Proc. of 12th Asian Regional Conf. on Soil Mech. and Geotechnical Eng.*, Keynote Paper, Singapore, **2**, 1157–1195.
- Bjerrum, L. (1967): Engineering geology of Norwegian normally consolidated marine clays as related to settlements of buildings, *Geotechnique*, **17**(2), 81–118.
- Dafalias, Y. (1982): Bounding surface elastoplasticity-viscoplasticity for particulate cohesive media, *Proc. of UTAM Conference on Deformation and Failure of Granular Materials*, Delft, 97–107.
- Hashiguchi, K. and Ueno, M. (1977): Elasto-plastic constitutive laws for granular materials, constitutive equations for soils, *Proc. of Specialty Session 9, 9th International Conf. on Soil Mech. and Foundation Eng.*, 73–82.
- Hashiguchi, K. (1980): Constitutive equation of elastoplastic materials with elasto-plastic transition, *Jour. of Appli. Mech.*, ASME, **102**(2), 266–272.
- Hashiguchi, K. and Okayasu, T. (2000): Time-dependent elastoplastic constitutive equation based on the subloading surface model and its application to soils, *Soils and Foundations*, **40**(4), 19–36.
- Kaneda, K. (1999): A modeling of elastoplastic behavior of structured soils and analysis of time-dependent like behavior of saturated soils by soil-water coupled computation, *Dissertation of Doctor of Engineering*, Nagoya University, 125–126 (in Japanese).
- Katona, M. G. (1984): Evaluation of viscoplastic cap model, *J. Geotech. Eng., Proc.*, ASCE, **110**(8), 1106–1125.
- Ladd, C. C., Foott, R., Ishihara, K. and Poulos, H. G. (1977): Stress-deformation and strength characteristics, *Proc. of 9th International Conf. on Soil Mech. and Foundation Eng.*, Tokyo, **1**, 421–494.
- Leonards, G. A. and Girault, G. A. (1961): A study of the one-dimensional consolidation test, *Proc. of 5th International Conf. on Soil Mech. and Foundation Eng.*, **1**, 213–218.
- Leroueil, S., Kabbaj, M., Tavenas, F. and Bouchard, R. (1985): Stress-strain-strain rate relation for the compressibility of sensitive natural clays, *Geotechnique*, **35**(2), 159–180.
- Nakai, T. and Mihara, Y. (1984): A new mechanical quantity for soils and its application to elastoplastic constitutive models, *Soils and Foundations*, **24**(2), 82–94.
- Nakai, T. and Matsuoka, H. (1986): A generalized elastoplastic constitutive model for clay in three-dimensional stresses, *Soils and Foundations*, **26**(3), 81–98.
- Nakai, T. (1989): An isotropic hardening elastoplastic model for sand considering the stress path dependency in three-dimensional stresses, *Soils and Foundations*, **29**(1), 119–137.
- Nakai, T. and Hinokio, T. (2004): A simple elastoplastic model for normally and over consolidated soils with unified material parameters, *Soils and Foundations*, **44**(2), 3–70.
- Nakai, T. (2007): Modeling of soil behavior based on  $t_{ij}$  concept, *Proc. of 13th Asian Regional Conf. on Soil Mech. and Geotechnical Eng.*, Keynote Paper, **2**, 69–89.
- Nakai, T., Kyokawa, H., Kikumoto, M. and Zhang, F. (2009a): Elastoplastic modeling of geomaterials considering the influence and density and bonding, *Proc. of Prediction and simulation methods for geohazard mitigation*, Kyoto, 367–373.
- Nakai, T., Shahin, H. M., Kikumoto, M., Kyokawa, H. and Zhang, F. (2009b): Simple and unified method for describing various characteristics of geomaterials, *Journal of Applied Mechanics JSCE*, **19**, 371–382 (in Japanese).
- Nakai, T., Shahin, H. M., Kikumoto, M., Kyokawa, H., Zhang, F. and Farias, M. M. (2011): A simple and unified three-dimensional model to describe various characteristics of soils, *Soils and Foundations*, **51**(6), 1149–1168.
- Nakano, M., Asaoka, A. and Constantinescu, D. T. (1998): Delayed compression and progressive failure of the assemble of crushed mudstone due to slaking, *Soils and Foundations*, **38**(4), 183–194.
- Nova, R. (1982): A viscoplastic constitutive model for normally consolidated clay, *Proc. of IUTAM Conference on Deformation and Failure of Granular Materials*, Delft, 287–295.
- Oshima, A., Ikeda, Y. and Masuda, S. (2002): Effects of load increment ratio on step loading consolidation test of clay, *Proc. of 37th Annual Meeting on JGS*, **1**, 289–290 (in Japanese).
- Perzyna, P. (1963): The constitutive equations for rate sensitive plastic materials, *Quart. Appli. Math.*, **20**(4), 321–332.
- Schofield, A. N. and Wroth, C. P. (1968): *Critical State Soil Mechanics*, McGraw-Hill, London.
- Sekiguchi, H. (1977): Rheological characteristics of clays, *Proc. of 9th International Conf. on Soil Mech. and Foundation Eng.*, **1**, 289–292.
- Sekiguchi, H. and Toriihara, M. (1976): Theory of one-dimensional consolidation of clays with consideration of their rheological properties, *Soils and Foundations*, **16**(1), 27–44.
- Sekiguchi, H. (1985): Macrometric approaches—static—intrinsically

time-dependent, *Proc. of Discussion Session on Constitutive laws of Soils, 11th International Conf. on Soil Mech. and Foundation Eng.*, 66-98.

- 33) Tanaka, H., Udaka, K. and Nosaka, T. (2006): Strain rate dependency of cohesive soils in consolidation settlement, *Soils and Foundations*, 46(3), 315-322.
- 34) Watabe, Y., Udaka, K. and Morikawa, Y. (2008): Strain rate effect on long-term consolidation of Osaka bay clay, *Soils and Foundations*, 48(4), 495-509.
- 35) Watabe, Y., Emura, T., Yamaji, T., Udaka, K. and Watanabe, Y. (2009): A consideration on upper limit of applied load in long term consolidation tests, *Proc. of 64th Annual Meeting on JSCE*, III-011, 21-22 (in Japanese).
- 36) Yoshikuni, H., Moriawaki, T., Ikegami, S. and Tajima, S. (1990), The effect of stress history on the secondary compression characteristics of over consolidated clay, *Proc. of 25th annual meeting on JGS*, 1, 381-382 (in Japanese).
- 37) Zhang, F., Yashima, A., Nakai, T., Ye, G. L. and Aung, H. (2005): An elasto-viscoplastic model for soft sedimentary rock based on  $t_{ij}$  concept and subloading surface, *Soils and Foundations*, 45(1), 65-73.

### APPENDIX I: LOADING CONDITION USING INCREMENT OF TOTAL VOID RATIO AND EXPLICIT EXPRESSION OF THE PROPOSED STRESS-STRAIN RELATION

In the elastoplastic region, the increments of elastic and plastic void ratios are given by Eqs. (9) and (26).

$$d(-e)^e = \kappa \frac{d\sigma}{\sigma} \quad (\text{A1; 9 bis})$$

$$d(-e)^p = \frac{(\lambda - \kappa) \frac{d\sigma}{\sigma} + d\psi}{1 + G(\rho) + Q(\omega)} \quad (\text{A2; 26 bis})$$

The stress increment  $d\sigma$  is expressed as follows using the increments of total void ratio and the plastic change in void ratio:

$$d\sigma = \frac{\sigma}{\kappa} d(-e)^e = \frac{\sigma}{\kappa} \{d(-e) - d(-e)^p\} \quad (\text{A3})$$

Substituting Eq. (A3) into Eq. (A2) and rearranging it, the following expression is obtained:

$$d(-e)^p = \frac{(\lambda - \kappa)d(-e) + \kappa d\psi}{\lambda + \kappa G(\rho) + \kappa Q(\omega)} \quad (\text{A4})$$

Usually the denominator of the above equation is positive, so that the loading condition is expressed as

$$\begin{cases} d(-e)^p \neq 0: & \text{if } (\lambda - \kappa)d(-e) + \kappa d\psi > 0 \\ d(-e)^p = 0: & \text{otherwise} \end{cases} \quad (\text{A5})$$

Substituting Eq. (A4) into Eq. (A3), the following incremental explicit stress-stress relation in elastoplastic region is obtained:

$$\begin{aligned} d\sigma &= \frac{(1 + G(\rho) + Q(\omega))\sigma}{\lambda + \kappa G(\rho) + \kappa Q(\omega)} d(-e) - \frac{\sigma}{\lambda + \kappa G(\rho) + \kappa Q(\omega)} d\psi \\ &= \frac{(1 + e_0)(1 + G(\rho) + Q(\omega))\sigma}{\lambda + \kappa G(\rho) + \kappa Q(\omega)} d\varepsilon \\ &\quad - \frac{\sigma}{\lambda + \kappa G(\rho) + \kappa Q(\omega)} d\psi \end{aligned} \quad (\text{A6})$$

The above equation becomes the stress-strain relation for stage II in the case of  $d\psi = 0$ , and it becomes the expression for stage I in the case of  $d\psi = 0$  and  $Q(\omega) = 0$ .

### APPENDIX II: MEANING OF PRESENT TIME-DEPENDENT MODEL, SIMILARITIES AND DIFFERENCES COMPARED TO SEKIGUCHI MODEL

Consider initially the one-dimensional behavior of non-structured normally consolidated soil without time effect. Its increment of plastic void ratio is given by Eq. (8)

$$d(-e)^p = (\lambda - \kappa) \cdot \frac{d\sigma}{\sigma} \quad (\text{A7; 8 bis})$$

In Fig. A1, the solid straight line (NCL) indicates the ideal  $e$ - $\ln \sigma$  relation of normally consolidated soil, and the arrows show schematically the stiffness at some points calculated by the subloading surface concept using the state variable  $\rho$ . The increment of plastic void ratio given by Eq. (17) according to the present model for an consolidated soil is given by:

$$d(-e)^p = \frac{\lambda - \kappa}{1 + G(\rho)} \cdot \frac{d\sigma}{\sigma} \quad (\text{A8; 17 bis})$$

As described before, it can be seen that positive values of  $\rho$  have the effect of increasing the stiffness, and negative values of  $\rho$  decrease the stiffness. Even if the initial void ratio is on the NCL ( $\rho = 0$ ) at point A, the void ratios in the subsequent calculation steps may stray from the NCL due to the numerical errors during calculations. For example, the stiffness calculated at point B becomes smaller than that on the NCL because of  $\rho < 0$ , and the stiffness calculated at point C becomes larger because of  $\rho > 0$ . So, the subloading surface concept is very useful not only to consider the influence of density but also to eliminate the accumulative errors during numerical calculations and converge to the ideal stress-stain curve automatically.

In the following, consider the modeling of the one-dimensional behavior of a non-structured normally consolidated soil with time effect. As shown in Fig. 16, it is assumed that the plastic change of void ratio is expressed as the summation of the component from I to J and the plastic component from J to P. This means that there ex-

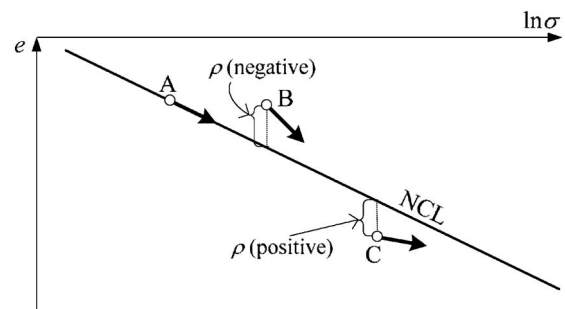


Fig. A1. Schematic diagram for explanation of stiffness for soils with positive and negative values of  $\rho$

ists a unique relation between void ratio, stress and rate of plastic void ratio change. When the initial and current values of void ratio, stress and rate of plastic void ratio change are denoted as  $(e_0, \sigma_0, (-\dot{e})_0^p)$  and  $(e, \sigma, (-\dot{e})^p)$ , the change of plastic void ratio is given by the following equation (Sekiguchi and Toriihara, 1976):

$$(-\Delta e)^p = e_0 - e - (-\Delta e)^e = (\lambda - \kappa) \ln \frac{\sigma}{\sigma_0} + \lambda_\alpha \ln \frac{(-\dot{e})_0^p}{(-\dot{e})^p} \quad (\text{A9})$$

By solving this ordinary differential equation with time variable, Sekiguchi (1977) obtained the plastic change of void ratio in the following form:

$$(-\Delta e)^p = \lambda_\alpha \ln \left\{ \frac{(-\dot{e})_0^p \cdot t}{\lambda_\alpha} \exp \left( \frac{F}{\lambda_\alpha} \right) + 1 \right\}$$

where

$$F = (\lambda - \kappa) \ln \frac{\sigma}{\sigma_0} \quad (\text{A10})$$

and the increment of plastic void ratio is calculated as

$$d(-e)^p = \frac{\partial(-\Delta e)^p}{\partial \sigma} d\sigma + \frac{\partial(-\Delta e)^p}{\partial t} dt \quad (\text{A11})$$

Sekiguchi (1977) defined the flow surface, which corresponds to the yield surface including time variable, by replacing  $F$  in Eq. (A10) with the Cam clay type yield function in three-dimensional stresses.

The meaning of the present modeling using the sub-loading surface concept for non-structured normally consolidated soil will be shown below. Although the basic assumption between void ratio, stress and rate of plastic void ratio change is the same as Sekiguchi's model, the plastic change of void ratio and the increment of plastic void ratio are expressed as follows from Eqs. (23) and (26):

$$(-\Delta e)^p = (\lambda - \kappa) \ln \frac{\sigma}{\sigma_0} + \rho - (\psi_0 - \psi) \quad (\text{A12})$$

$$d(-e)^p = \frac{(\lambda - \kappa) \frac{1}{\sigma} d\sigma + d\psi}{1 + G(\rho)} \quad (\text{A13})$$

Here, the state variable  $\rho$  is introduced and automatically corrects the stiffness of a normally consolidated soil. The state variable  $\psi$ , which determines the current position of NCL, and its increment  $d\psi$  are given by Eqs. (36) and (37) using the coefficient of secondary consolidation  $\lambda_\alpha$  and the rate of plastic void ratio change.

$$\begin{cases} \psi = -\lambda_\alpha \ln(-\dot{e})^p \\ \psi_0 = -\lambda_\alpha \ln(-\dot{e})_0^p \end{cases} \quad (\text{A14; 36 bis})$$

$$d\psi = \frac{\partial \psi}{\partial t} dt = (-\dot{e})^p dt \quad (\text{A15; 37 bis})$$

Here, the rate of plastic void ratio change  $(-\dot{e})^p$  in Eqs. (36) and (37) is determined from the plastic changes of void ratio, stress increment and time increment from the

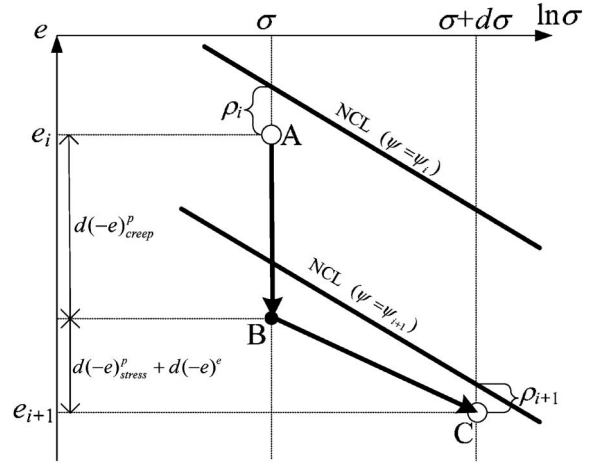


Fig. A2. Schematic diagram for explanation of incremental calculation by the time-dependent model

previous calculation step to the current calculation step and is used only to determine the position of the NCL and the increment  $d\psi$  for the next incremental calculation.

Figure A2 shows schematically the calculation process based on the present time-dependent model in the  $e$ - $\ln \sigma$  plane. The current condition ( $i$ th step) is represented with void ratio  $e = e_i$ , stress  $\sigma = \sigma$ , time  $t = t$ , rate of plastic void ratio change  $(-\dot{e})^p = (-\dot{e})_i^p$ , state variable  $\rho = \rho_i$  and the NCL with  $\psi_i$ . These variables in next condition ( $(i+1)$ th step) are represented as  $e_{i+1}$ ,  $\sigma + d\sigma$ ,  $t + dt$ ,  $(-\dot{e})_{i+1}^p$ ,  $\rho_{i+1}$  and the NCL with  $\psi_{i+1}$ . Here, the increment of void ratio from the  $i$ th step (point A) to the  $(i+1)$ th step (point C) is expressed as a summation of the component due to creep (A to B) and the component due to stress increment (B to C). Looking at Eqs. (A13) and (A15), these components are given by

$$d(-e)_{\text{creep}} = d(-e)_{\text{creep}}^p = \frac{(-\dot{e})^p dt}{1 + G(\rho_i)} \quad (\text{A16})$$

$$\begin{aligned} d(-e)_{\text{stress}} &= d(-e)_{\text{stress}}^p + d(-e)^e \\ &= \left\{ \frac{\lambda - \kappa}{1 + G(\rho_i)} + \kappa \right\} \frac{1}{\sigma} d\sigma \end{aligned} \quad (\text{A17})$$

Then, the rate of plastic void ratio change  $(-\dot{e})_{i+1}^p$  used in the following calculation step is determined as

$$\begin{cases} (-\dot{e})_{i+1}^p = \{e_i - e_{i+1} - d(-e)^e\} / dt \quad \text{or} \\ (-\dot{e})_{i+1}^p = \{d(-e)_{\text{creep}}^p + d(-e)_{\text{stress}}^p\} / dt \end{cases} \quad (\text{A18})$$

From Eq. (A14), the position of the NCL with  $\psi_{i+1}$  can be determined using the rate obtained by Eq. (A18), and the value of  $\rho_{i+1}$  can be defined as the difference between the void ratio  $e_{i+1}$  and that on the NCL with  $\psi_{i+1}$  at the same stress level. These are used in the subsequent calculation step. The errors which arise when using the previous values of the rate and not solving the differential equation are self-corrected by the state variable  $\rho$  in the same way as in the case without time effect, as mentioned before. Although it is possible to carry out iterative calculations so that  $(-\dot{e})_{i+1}^p \cong (-\dot{e})^p$ , there is not much difference between the results with and without iteration unless

employing large increments of stress and time.

For the case of over consolidated soils and structured soils,  $G(\rho)$  and  $Q(\omega)$  converge to zero with the development of plastic deformation and the void ratio finally becomes the same as that in normally consolidated soils. Therefore, determining the position of the NCL ( $\psi$ ) by the current rate of plastic void ratio change alone even in over consolidated soils and structured soils in the same way as that in normally consolidated soils, the model described here can be applied to over consolidated soils and structured soils as well.

The validity of the present model has been verified by the simulations of various kinds of time-dependent tests of soils in this paper. It should be noted that although non stationary flow surface models such as Sekiguchi's model are useful for normally consolidated soils alone, the model includes the time variable which is non objective variable. The present models (Eqs. (36) to (39)) are applicable not only to normally consolidated soils but also to over consolidated soils and structured soils, and they are also objective as the time variable is not included.